Cretaceous Research 120 (2021) 104725

Contents lists available at ScienceDirect

Cretaceous Research

journal homepage: www.elsevier.com/locate/CretRes

The Campanian–Maastrichtian interval at The Naze, James Ross Island, Antarctica: microbiostratigraphic and paleoenvironmental study

Enelise Katia Piovesan [a, *], Osvaldo José Correia Filho [b], Robbyson Mendes Melo [a], Luiz Drude Lacerda [c], Rodolfo Otávio Dos Santos [d], Allysson Pontes Pinheiro [e], Fabiana Rodrigues Costa [f], Juliana Manso Sayão [g], Alexander Wilhelm Armin Kellner [h]

[a] Laboratório de Micropaleontologia Aplicada / LAGESE / LITPEG, Universidade Federal de Pernambuco, Recife, Pernambuco, Brazil
[b] Programa de Pós-graduação Geociências, Departamento de Geologia, Universidade Federal de Pernambuco, Pernambuco, Brazil
[c] Instituto de Ciências Do Mar, LABOMAR, Universidade Federal do Ceará, Fortaleza, Ceará, Brazil
[d] Laboratório de Herpetologia e Paleontologia da USP, Instituto de Biociências, Universidade de São Paulo, São Paulo, Brazil
[e] Laboratório de Crustáceos do Semiárido (LACRUSE), Universidade Regional do Cariri, Crato, Ceará, Brazil
[f] Laboratório de Paleontologia de Vertebrados e Comportamento Animal (LAPC), Universidade Federal do ABC, São Bernardo do Campo, São Paulo, Brazil
[g] Laboratório de Paleobiologia e Paleogeografia Antártica, Museu Nacional, Universidade Federal do Rio de Janeiro, Rio de Janeiro, Brazil
[h] Laboratório de Sistemática e Tafonomia de Vertebrados Fósseis, Departamento de Geologia e Paleontologia, Museu Nacional, Universidade Federal do Rio de Janeiro, Rio de Janeiro, Brazil

ARTICLE INFO

Article history:
Received 17 April 2020
Received in revised form
25 November 2020
Accepted in revised form 27 November 2020
Available online 6 December 2020

Keywords:
Agglutinated foraminifera
Paleoecology
Biostratigraphy
Hg-TOC stratigraphy
Campanian–Maastrichtian

ABSTRACT

A biostratigraphic and paleoenvironmental characterization of the Campanian–Maastrichtian deposits on The Naze (James Ross Island, Antarctica) based on the foraminiferal assemblages, lithofacies analysis, and Hg/total organic carbon (TOC) data was developed. The sedimentary deposits mapped in The Naze region showed an association of four sedimentary lithofacies, including greenish-gray claystone, shales with levels of concretion, bioturbated marl, and sandstone. The sedimentary deposits have been covered by a fifth lithofacies, the James Ross Island Volcanic Group (JRIVG), which consists of pyroclastic rocks interbedded with basalt bodies. The association of agglutinated foraminifera was found to consist mainly of *Rzehakina epigona, Trochammina ribstonensis, Gaudryina healyi, Karreriella aegra, Dorothia elongata, Alveolophragmium macellarii, Cyclammina complanata* and *Spiroplectammina spectabilis*, that allow to infer a Campanian–early Maastrichtian age to the studied interval. An association of opportunistic agglutinated foraminifera predominated in this stressful environment. The absence of Hg-TOC unassociated excursions ruled out distal volcanism as a source of environmental stress, while Hg/TOC ratio variability suggested that regional oceanic processes were the major environmental change driver.

1. Introduction

The James Ross Archipelago consists of a group of islands located near the Antarctic Peninsula (63.76°S – 64.58°S, 56.44°W – 58.50°W), and covers an area of ~2600 km^2 (Del Valle and Scasso, 2004). The Naze is included in the James Ross Basin (JRB) (Riding, 1996; Crame et al., 1996), and comprises an important Upper Cretaceous section (Fig. 1).

The Campanian–Maastrichtian (~83–66 Ma) was a time of global climate cooling (Jenkyns et al., 1994; Huber et al., 2002; Friedrich et al., 2009, 2012; Linnert et al., 2018). The culmination of this event was accompanied by third-order global sea level falls (e.g., Haq et al., 1987; Barrera et al., 1997; Li and Keller, 1999), and several significant carbon-cycle perturbations (Barrera et al., 1997). These phenomena were associated with the so-called Campanian–Maastrichtian Boundary Event (CMBE; Friedrich et al., 2009), and formally defined by the first appearance of the

* Corresponding author.
E-mail addresses: katiapiovesan@gmail.com (E.K. Piovesan), osv.correia@yahoo.com.br (O.J. Correia Filho), robbysonmelo@gmail.com (R.M. Melo), ldrude1956@gmail.com (L.D. Lacerda), rodolfosantos013@gmail.com (R.O. Dos Santos), allysson.pinheiro@urca.br (A.P. Pinheiro), fabiana.costa@ufabc.edu.br (F.R. Costa), jmsayao@gmail.com (J.M. Sayão), kellner@mn.ufrj.br (A.W. Armin Kellner).

https://doi.org/10.1016/j.cretres.2020.104725
0195-6671/

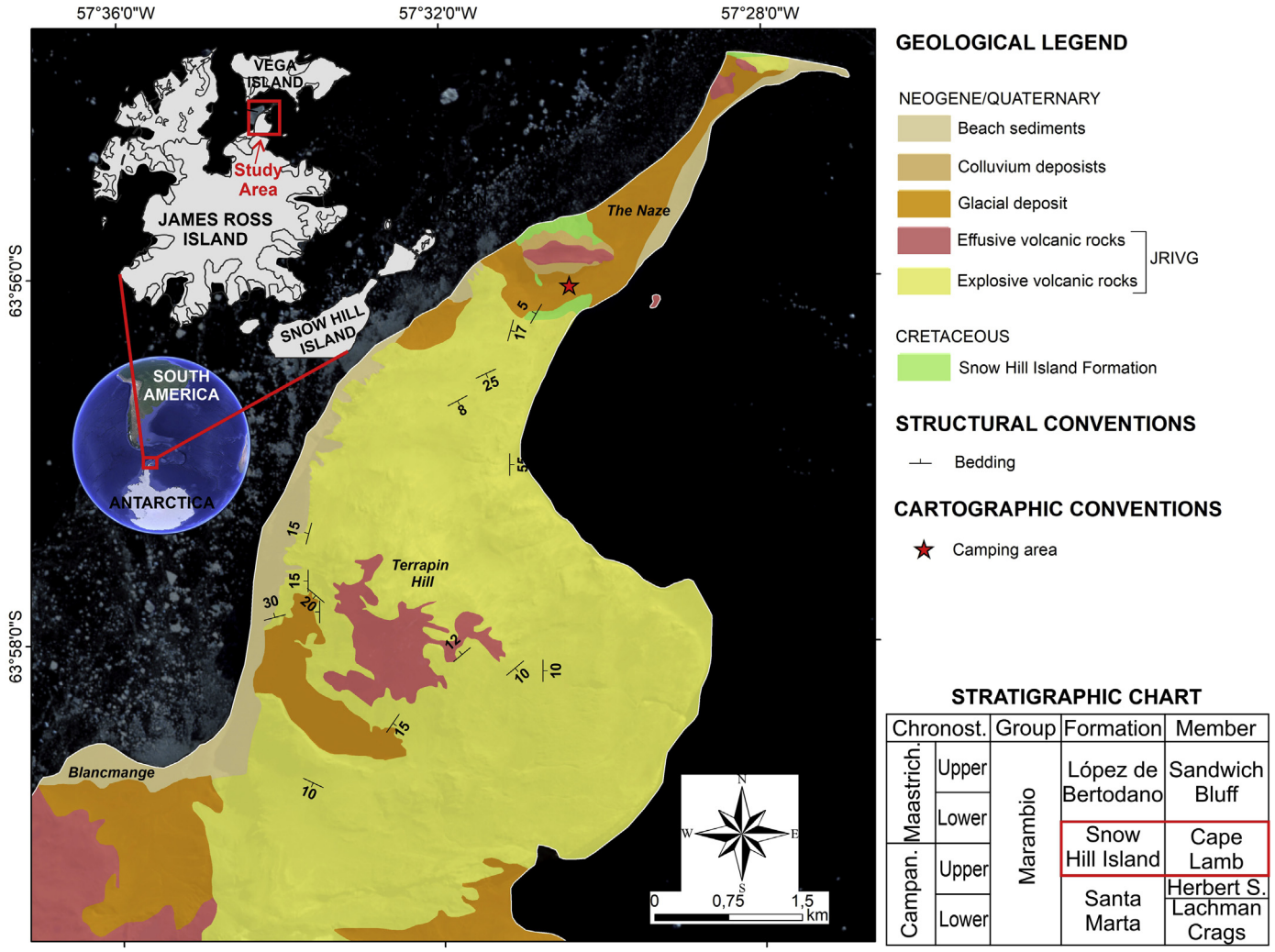

Fig. 1. Geological map of The Naze, James Ross Island, based on collected field data and Sentinel satellite imagery. Detail for the simplified stratigraphic chart of the JRB, showing the studied deposit belonging to the Snow Hill Island Formation (SHIFM), after Olivero (2012).

ammonite *Pachydiscus neubergicus*, which delimits the base of Maastrichtian strata (Odin et al., 1996; Ogg et al., 2016).

In the JRB, the Campanian–Maastrichtian interval has been identified based on the stratigraphic distribution of macrofossils, especially ammonoids and microfossils (Del Valle et al., 1982; Crame et al., 1991; Pirrie et al., 1991, 1997; Olivero and Medina, 2000; Olivero, 2012; Di Pasquo and Martin, 2013; Guerra et al., 2015; Amenábar et al., 2019). The base of the Maastrichtian Stage was isotopically reassessed by Crame et al. (1999), using the strontium isotopes $^{87}Sr/^{86}Sr$, on Vega, Snow Hill, Seymour, and James Ross islands. Results from a magnetostratigraphic study by Milanese et al. (2019), on sedimentary rocks of the Marambio Group, in the SE JRB, indicated a mid-Campanian–early Maastrichtian age for the studied deposits, which partially agreed with previous ammonite data.

Considering Upper Cretaceous foraminifera from James Ross Island (JRI), some studies have shown a diverse assemblage, composed of benthic and planktic species from marginal marine to bathyal environments (Macfadyen, 1966; Webb, 1972; Huber, 1988; Morlotti and Concheyro, 1999; Hradecká et al., 2011; Florisbal et al., 2013; Caramés et al., 2016). In biostratigraphic terms, the Campanian–Maastrichtian section was dated by recognizing the *Gaudryina healyi* Zone (mid to late Campanian), which allowed correlation to be established between the Cape Lamb (Vega Island), The Naze (JRI), Snow Hill Island, and lowermost Seymour Island beds. In contrast, the late Campanian through Maastrichtian *Hedbergella monmouthensis* Zone has been reported only from Seymour Island (Huber, 1988). In the study described here, analyses of foraminiferal assemblages, sedimentary lithofacies, and Hg/total organic carbon (TOC) data, derived from the Campanian–Maastrichtian sedimentary record at The Naze in the JRB, were combined, to improve regional biostratigraphic and paleoenvironmental characterization.

2. Geological setting

The JRB is located in the northern region of the Antarctic Peninsula (Fig. 1). Its geological evolution is complex and is related to Mesozoic retro-arc basins (Hathway, 2000; Del Valle and Scasso, 2004). The JRB has sedimentary strata approximately 6000 m thick, ranging from the Lower Cretaceous (Barremian) to the Paleogene (Eocene) (Milanese et al., 2019).

The Cretaceous infill of the JRB is divided into two stratigraphic units, the Gustav Group, ranging from the Aptian to the Coniacian, and the Marambio Group, comprising the Santonian–Danian interval (Olivero, 2012; Amenábar et al., 2019), and consisting of fine

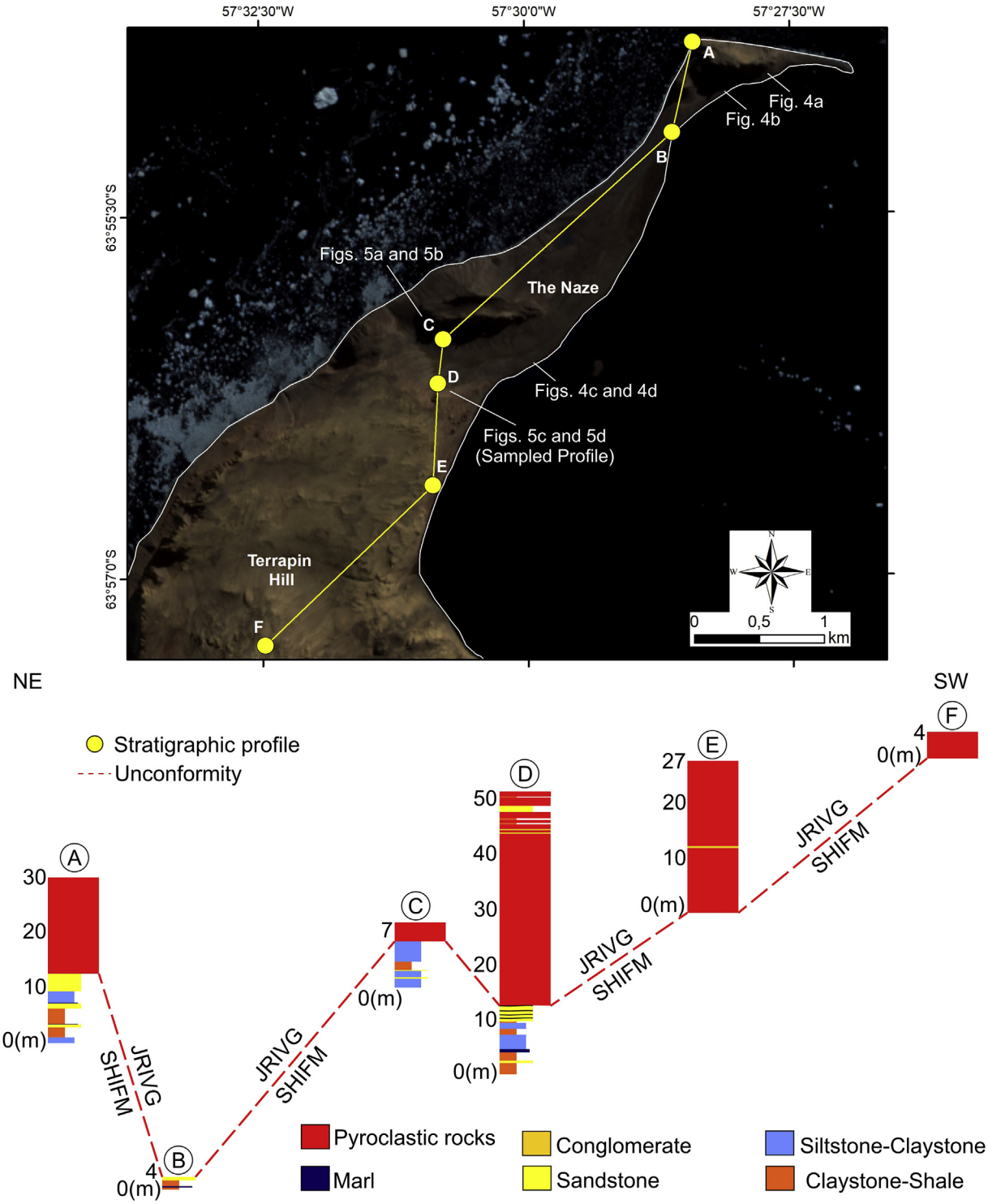

Fig. 2. Sentinel satellite (*Sentinel-2*) imagery showing the lithostratigraphy correlation through The Naze from stratigraphic profiles acquired. The yellow line represents the lithological correlations for the sections (A–E) detailed in the lower portion of this figure. The dashed red line demonstrates the regional unconformity between the top of the sedimentary units related to Snow Hill Island Formation (SHIFM) and the James Ross Island Volcanic Group (JRIVG). (For interpretation of the references to colour in this figure legend, the reader is referred to the Web version of this article.)

sandstones, claystones and carbonates. This facies association may indicate shallow marine sedimentation in a transitional marine environment (Rinaldi et al., 1978; Crame et al., 1991; Pirrie et al., 1997; Olivero and Medina, 2000; Francis et al., 2006; Olivero, 2012; Guerra et al., 2015). The Snow Hill Island Formation is composed of sandstone, mudstone and a mudstone–siltstone-dominated heterolytic layers (Olivero, 2012; O'Gorman, 2012). The Snow Hill Island Formation deposits have been covered by lava flows and pyroclastic rocks from the James Ross Island Volcanic Group - JRIVG (Calabozo et al., 2015), aged 6.2–0.13 Ma

(Kristjansson et al., 2005; Calabozo et al., 2015), and by glacial deposits (Fig. 1).

Crame et al. (1991) and Crame (1992) presented a Campanian–Maastrichtian stratigraphic summary of the Upper Cretaceous for the JRB, combining stratigraphic data for dinoflagellates, ammonoids, and other invertebrate fossils. Crame et al. (2004) presented an integrated study of Antarctica lithology, biostratigraphy and chronostratigraphy, dealing with the Maastrichtian.

3. Material and methods

The studied material was collected by the PALEOANTAR Project (Kellner et al., 2019) in the region of The Naze, JRI, in the austral summer of 2017/2018, during the 36th Antarctic Operation (OPERANTAR XXXVI), supported by the Brazilian Antarctic Program (PROANTAR).

Geological mapping was carried out at 1:30,000 scale, and five stratigraphic sections were made in the study area. From the stratigraphic profiles described here, the best exposed was selected (Fig. 2, profile D, located at 63.9° S and 57.5° W), and then sampled for micropaleontological and geochemical analyses. Geologic mapping was created using images provided by the Sentinel-2 satellite and field data (Figs 1–2). From the 13 spectral bands of this satellite, the red, green, and blue bands were combined, to produce a false-color image, with a 10 m spatial resolution.

A total of 23 samples were processed but only 10 of them resulted productive for microfossils. Preparation followed the usual procedure for carbonate microfossil recovery. Approximately 100 g of rocks were immersed in hydrogen peroxide, and then washed under water in 45, 63, 180, 250 and 500 μm sieves. All specimens from the 180 and 250 μm fractions were selected, with the remaining fractions being barren. The relative abundance of foraminifera species was calculated from the total count recovered in each sample, and the distribution of agglutinated foraminiferal morphogroups was used as an indicator of paleoenvironmental conditions (according to Jones and Charnock, 1985; Koutsoukos and Hart, 1990; Nagy et al., 1995; van den Akker et al., 2000; Kaminski and Gradstein, 2005; Murray et al., 2011). The specimens presented here were deposited in the micropaleontological collection of the Laboratory of Applied Micropaleontology (LMA) of the Federal University of Pernambuco, Brazil.

The same samples used for micropaleontology analysis were used for the quantification of total mercury and TOC concentrations. Before Hg quantification, sediment samples were digested according to the method described in Aguiar et al. (2007). TOC was quantified according to the method of Yeomans and Bremner (1988), as adapted by Mendonça and Matos (2005).

4. Results

4.1. Lithofacies

The geological mapping of the rocks cropping out in The Naze Peninsula allowed identification of five lithofacies: four of them represent carbonate–siliciclastic sedimentary rocks which are related to the shallow marine environment, and the other lithofacies related to volcanic–pyroclastic sequences that cover the Upper Cretaceous sedimentary lithofacies (Fig. 3). Sedimentary lithofacies occur in a restricted area in the The Naze, whereas the outcrops of the JRIVG are widely distributed in the mapped region. The JRIVG is represented by sequences of pyroclastic deposits interlayered with effusive volcanic rocks of basic composition. From the stratigraphic profiles, it was possible to verify that the contact at the top of the Cretaceous rocks (Snow Hill Island Formation) occurred through an erosive unconformity, which marked the beginning of JRIVG deposition.

The mapped sedimentary units were divided into four lithofacies, as illustrated in Figs 4 and 5. The first mapped lithofacies was given the abbreviation MSht, and presented good lateral continuity in the studied area; it consisted of mudstones, represented by silt and clay, interbedded with fine sandstones, generating a parallel, heterolithic lamination. Fossil concretions that contained abundant marine crustaceans, as well as flaser, wavy, and linsen sedimentary structures, were also found in this lithofacies. MSht

Facies	Lithologic Association	Main Sedimentary Processes (interpretation)
Sgn	Medium-to fine sandstone with normal grading, cross-bedding stratification claystone drape and concretions	Cohesive gravitational deposit of sands related to turbulent flows
MSht	Claystone and siltstone interbeeding with fine sandstone, heterolithic lamination with concretions and wavy and lisen structures	Subaqueous migration of sand waves with bedload sediments; suspended load (clays) and traction (sands)
Mb	Marls and claystone with bioturbation	Decantation of clay and carbonates
Ml	Fossiliferous shale and claystone with planar lamination and concretions	Decantation of clay and organic matter in anoxic subaqueous environment
JRIVG	James Ross Volcanic Group	Effusive and explosive magmatism

Fig. 3. Lithofacies identified in the study area. Four of them are sedimentary lithofacies and the fifth is related to volcanic deposits of the JRIVG.

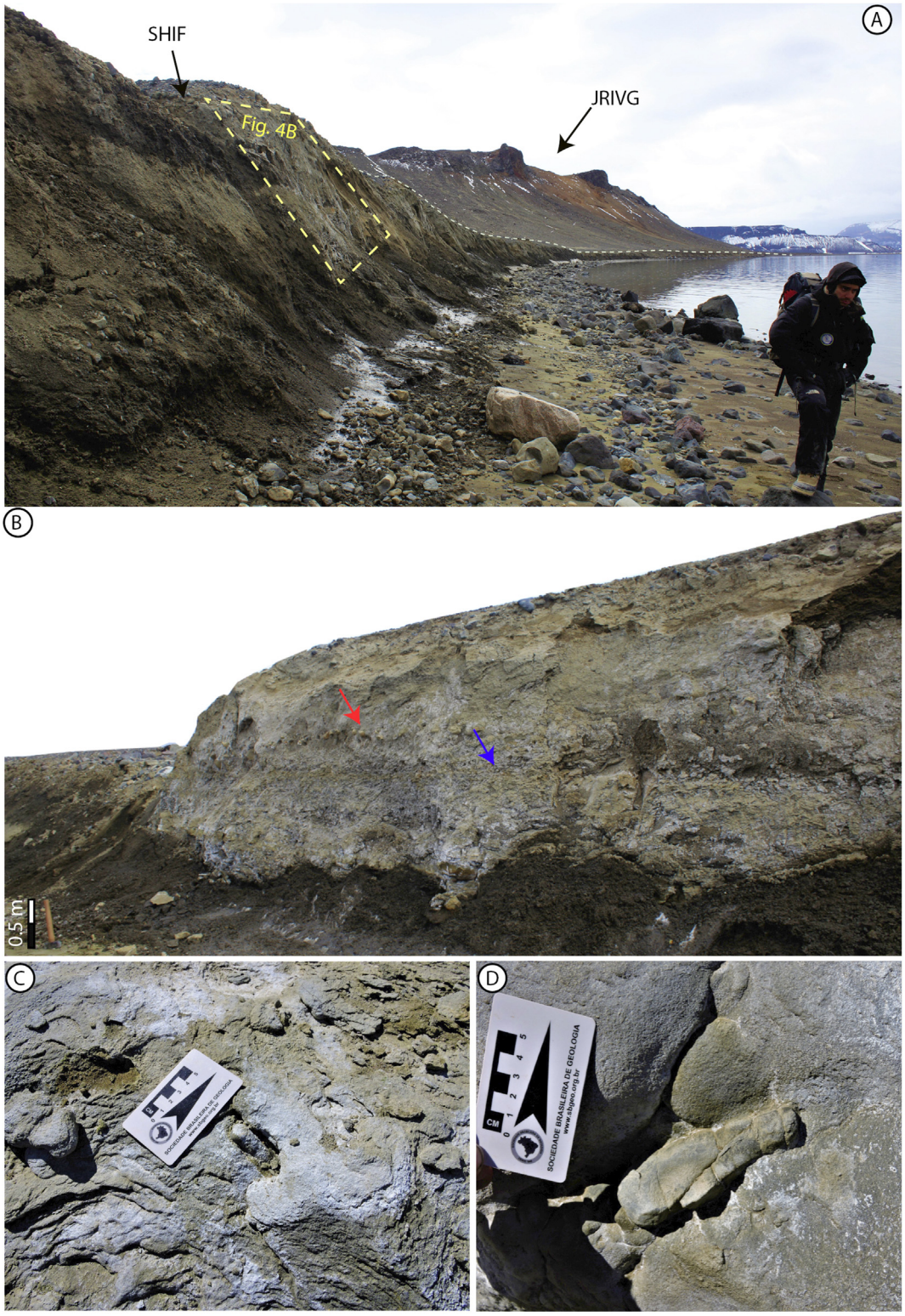

Fig. 4. Photographs of the lithofacies mapped on The Naze: A The dotted white lines mark contact between the Sgn lithofacies from the SHIFM and the JRIVG; B detail of the erosive levels (blue and red arrows) inserted in Sgn lithofacies. Blue and red arrows indicate a level of reworked clay clasts and concretions, respectively (scale = 0.5 m); C Mb lithofacies showing parallel bioturbation and flat lamination; D Mb lithofacies bioturbation detail. (For interpretation of the references to colour in this figure legend, the reader is referred to the Web version of this article.)

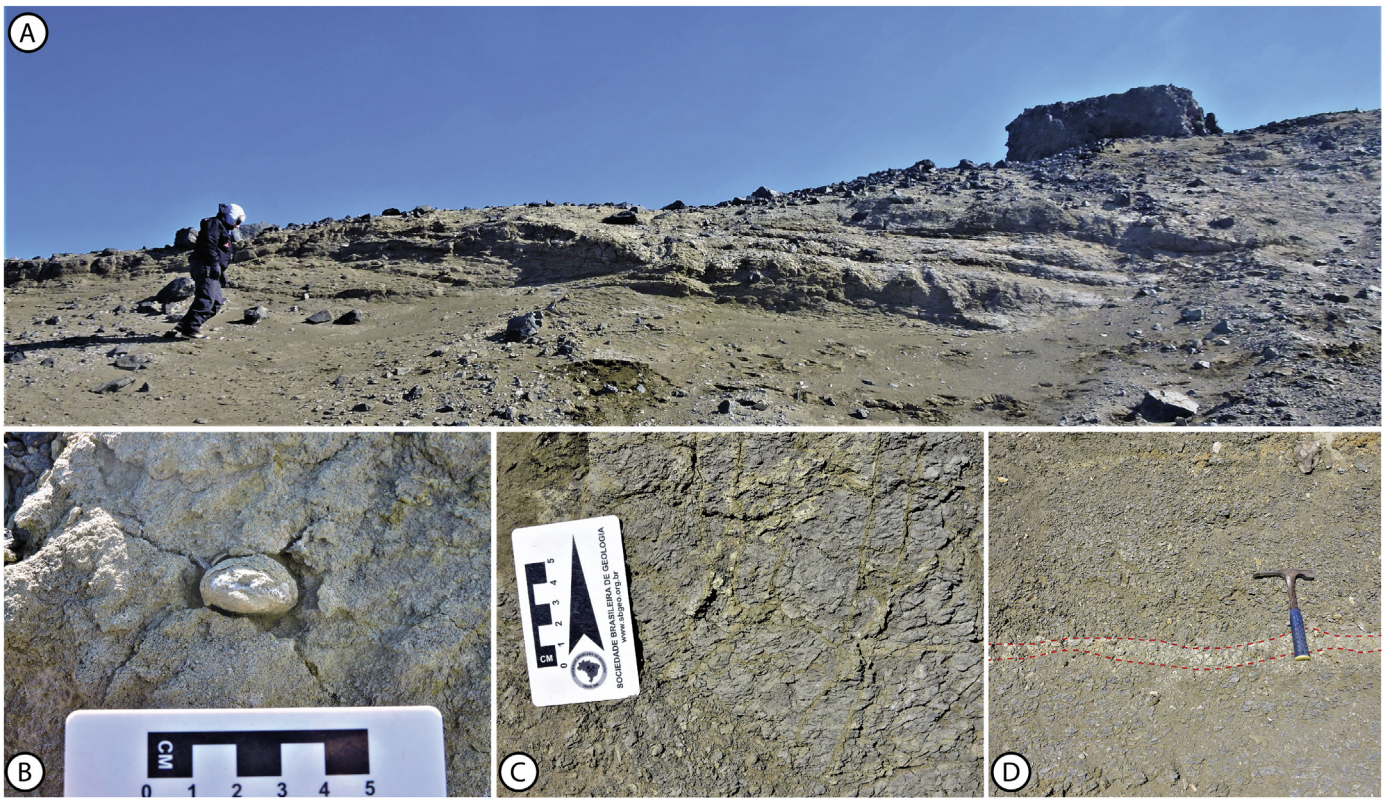

Fig. 5. Series of photos showing the main features mapped at The Naze. A Detail for the heterolithic level: MSht lithofacies, composed of interbedded fine pelites and sandstones, with heterolithic lamination; B heterolithic level, with a calcitic concretion, and MSht lithofacies (scale = 5 cm); C Ml lithofacies: greenish shale showing fissility and late fractures with oxidized planes (scale = 5 cm); D from the base of the MSht lithofacies: the red dotted lines indicate a layer of Mb lithofacies, with Ml lithofacies above. (For interpretation of the references to colour in this figure legend, the reader is referred to the Web version of this article.)

can be interpreted as a result of transport energy oscillations, which cause transport in the sand fraction, together with decantation and/or clay transport, producing the sedimentary structures observed in the outcrops.

A second lithofacies (defined as Mb) appeared as thin marl layers with bioturbation, and presented a discontinuous parallel lamination, representing an abrupt change in depositional conditions. There was a predominance of chemical–biological carbonate precipitation, together with periods of low energy, in which the clay decantation process dominated.

The third lithofacies (Ml) consisted of greenish and fossiliferous shales, with carbonate concretions and scattered fossil fragments in its matrix. The laminations were parallel and generally presented good lateral continuity, despite its presents local deformation due to JRIVG intrusions. The Ml lithofacies indicated a low energy condition, together with a predominance of pelitic material decantation in deep water and low oxygenation conditions, as witnessed by the presence of fine pyrite grains.

The fourth lithofacies (Sgn) consisted of a medium-to-fine, beige-colored sandstone layer, with normal and multiple gradations that contained a level of reworked clay clasts and concretions. The lower contact between the Sgn lithofacies and Ml is erosive, which was, perhaps, marking a local unconformity. Sgn lithofacies could be interpreted as a traction product, related to underwater gravitational flows.

There was a fifth lithofacies capping the four described above, related to volcanic–pyroclastic units of the JRIVG (Fig. 4), which occurs almost throughout the region of The Naze Peninsula. These are pyroclastic rocks, classified as ignimbrites, and surge deposits (Ghidella et al., 2013), with the latter making up the main substrates of Terrapin Hill.

4.2. Foraminiferal assemblages

In the present study, only 10 out of the 23 analyzed samples yielded microfossils (Figs 2 and 6, section D), and these consisted of an abundant Upper Cretaceous (Campanian–Maastrichtian) foraminiferal assemblage. Although the specimens were only poorly to moderately preserved, 38 benthic foraminifera taxa were identified, and these taxa included 37 agglutinated and a single calcareous species (Fig. 6 and supplementary material). No planktic species were recovered. Photomicrography of representative specimens from each taxon has been presented in Figs 7–9.

Some specimen tests were found in a flat condition (*Trochammina, Alveolophragmium* and *Reophax*), and others fragmented (mainly the elongated tubular forms). Throughout the section where foraminifera were recorded (samples PA29.1–11), only sample PA29.6 was barren, with all others dominated by agglutinated foraminifera. The rare calcareous specimens, attributed to the genus *Anomalinoides*, had an opaque appearance, with signs of dissolution. These specimens were confined at the top of the section, and represented an impoverished and dissolution-resistant association, which suggested a period of low calcium carbonate availability in the water column and/or the water/sediment interface. Foraminifera were not found in the upper section (samples PA29.12–23).

Morphogroup analyses (Fig. 10) showed that the assemblage compositions varied, with morphogroups M4a (epifaunal/shallow infaunal, rounded plane form) and M2b (epifaunal plano–convex trochospiral form) more abundant in these assemblages. There was an increase in the relative abundance of infauna from the middle portion of the section (sample P29.8), represented by morphogroups M2a (globular form) and M4b (elongated form).

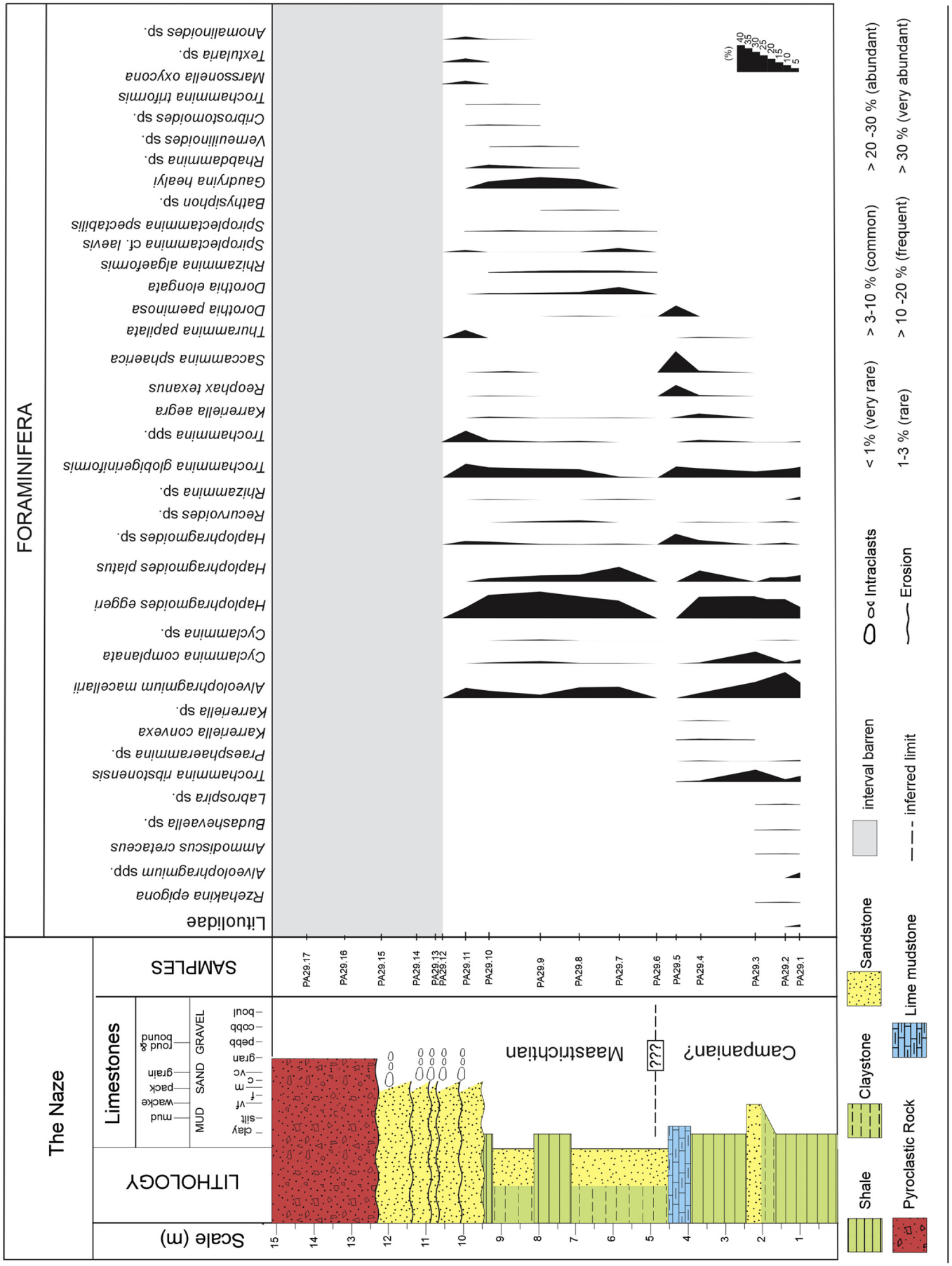

Fig. 6. Distribution of recovered foraminifera from The Naze, section D.

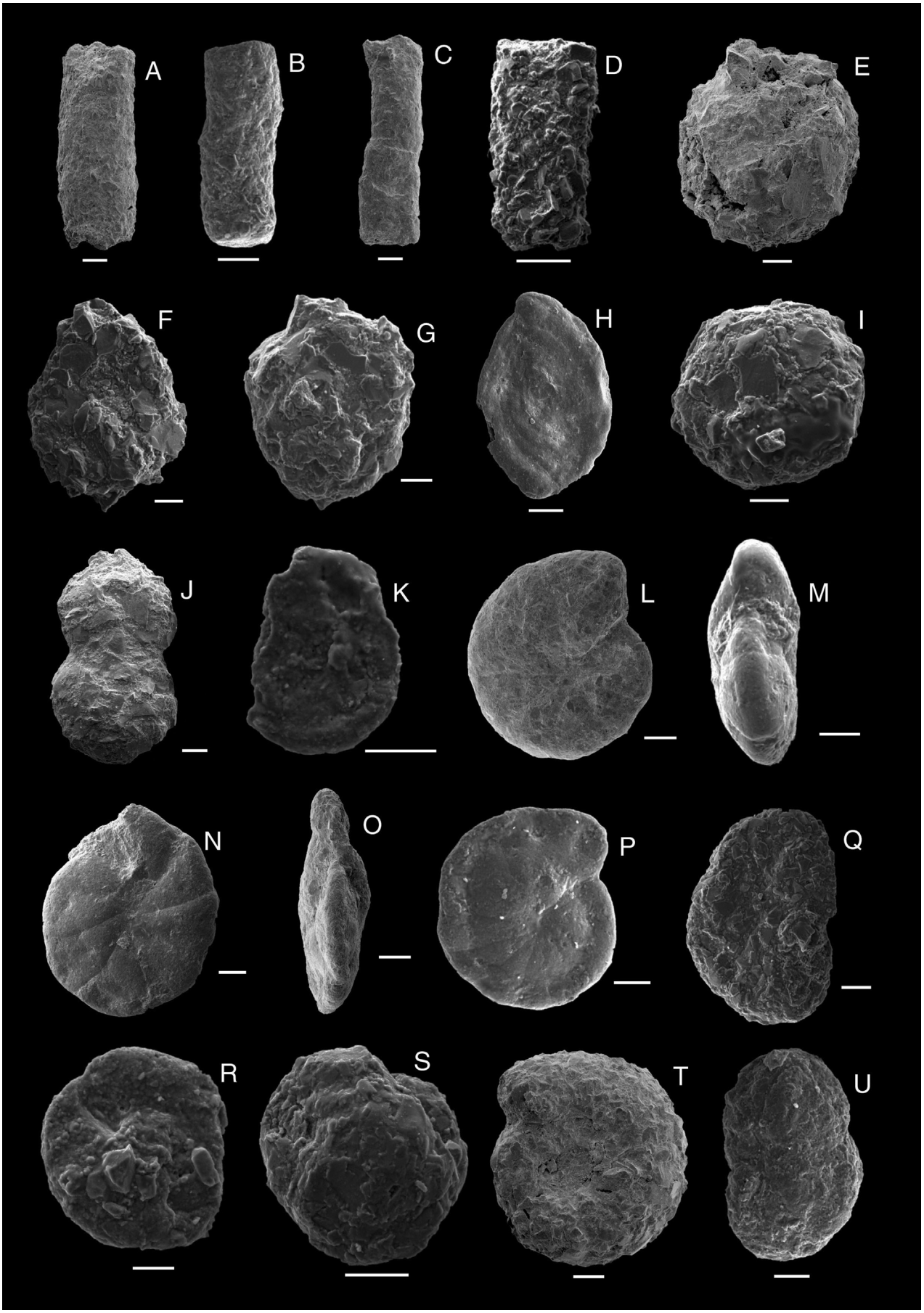
A
B
C
D
E
F
G
H
I
J
K
L
M
N
O
P
Q
R
S
T
U

Morphogroups M1 (tubular form) and M2c (elongate keeled form) occurred only from the middle portion of the section (sample PA29.7), while M3a (flattened planispiral form) occurred only at the base of the section (sample PA29.2)—and in low abundance. As for the life position, epifaunal/shallow infaunal foraminifera dominated the associations, followed by the infaunal, which presented a dominance peak in sample P29.5.

4.3. Geochemical results

The basal portion of the studied section (Fig.11, samples PA29.1–4; and supplementary material) showed high Hg and TOC concentrations, resulting in a high Hg/TOC ratio. There was a sharp negative excursion of Hg and TOC concentrations, as well as of the Hg/TOC ratio, at the interface of samples PA29.5–6, which signaled decreased carbon and mercury transfers to the sediments. For the medium portion of the section (Fig.11, samples PA29.7–11), high values were recorded for both variables, although there was no anomalous peak in the Hg/TOC ratio. This could indicate significant influence from volcanogenic Hg, as observed in different time periods (see Sial et al., 2016, for a review), and there was no evidence for an Hg drawdown by organic carbon—which is a major Hg scavenging process for sediments. It was found that Hg concentrations were lower than would be typical for such peaks, such as in the K–Pg at Biddart section, France (~50 $ng.g^{-1}$) (Font et al., 2016), and at Stevns Klint section, Denmark (127–257 $ng.g^{-1}$) (Sial et al., 2013), during the latest Permian extinction (up to 600 $ng.g^{-1}$) (Sanei et al., 2012), and at the Toarcian Oceanic Anoxic Event (T–OAE) horizon, in which Hg concentrations reached 200–300 $ng.g^{-1}$ (Percival et al., 2015).

5. Discussion

5.1. Biostratigraphy

The Campanian–Maastrichtian boundary in Antarctica is defined by the range of the ammonite *Gunnarites antarcticus*, with the reference section located on Cape Lamb Peninsula, Vega Island (Crame et al., 1999). Campanian–Maastrichtian foraminiferal assemblages from JRI and surrounding areas have been the subject of several studies (Macfadyen, 1966; Huber et al., 1983; Huber, 1988; Morlotti and Concheyro, 1999; Caramés et al., 2016). In the JRI region, the foraminiferal biostratigraphic framework for the Late Cretaceous was first established by Huber (1988), who divided it into three biozones, a ?mid–late Campanian *Gaudryina healyi* Zone, a late Campanian–Maastrichtian *Hedbergella monmouthensis* Zone, and a Danian *Globastica daubjergensis* Zone.

The constraint of the age of the Snow Hill Island Formation deposits at The Naze has been a matter of debate. Previous studies here, carried out by Askin (1988) and Huber (1988) documented palynomorphs and foraminiferal assemblages which they attributed to the mid–late Campanian. Subsequently, Bowman et al. (2012) revised the dinoflagellate assemblages from the López de Bertodano Formation on Seymour Island, previously analyzed by Askin (1988), and proposed a new biozonation, positioning these deposits in the late Maastrichtian. More recently, outcrops from The Naze were assigned to the early Maastrichtian, by Di Pasquo and Martin (2013), although the authors reported several palynomorphs, mainly from the Campanian–Maastrichtian. They supported the early Maastrichtian age due to the presence of the ammonoid *Kitchinites darwinii*, recovered approximately 20 m above the base of the section, but the lowest level showed a palynological association in a close relationship with Campanian taxa.

The global stratigraphic range of species from our material revealed that several, long-ranging Late Cretaceous taxa have been reported from the late Campanian–Maastrichtian deposits in Europe, North America, Mexico, South America, Australia and New Zealand (Table 1). Based on the distribution of our foraminiferal assemblage, it was possible to divide the section into two portions, related to the Campanian–early Maastrichtian interval (Fig. 6). The lower portion (samples PA29.1–6) probably represented the Campanian age, as supported by the occurrence of *Trochammina ribstonensis, Karreriella convexa, Ammodiscus cretaceus, Rzehakina epigona, Praesphaerammina* sp. and *Budashevaella* sp. Although the genus *Rzehakina* has been reported from the Campanian to the Eocene (Serova, 1969; Kaminski et al., 1988; Bolli et al., 1994; Malumián and Jannou, 2010), the first occurrence of *R. epigona* was recorded in the late Campanian of the *Globotruncanita calcarata* Zone (Scott, 1961; Kostka, 1993; Bak, 2000). In the JRI region, *R. epigona* was considered diagnostic of the *Gaudryina healyi* Zone (Huber, 1988)—which was first described from the Haumurian Stage (lower Campanian to upper Maastrichtian) in New Zealand (Webb, 1971, 1973; Crampton et al., 2000). *Trochammina ribstonensis* was also reported from the late Santonian and early Maastrichtian (Wall, 1967), and from the Santonian–Campanian (Nauss, 1947; Tappan, 1962; Mello, 1971; Caldwell and North, 1984).

The upper portion of the studied section (samples PA29.7–11) was related to the lower Maastrichtian (Fig. 6). It was characterized by the first recorded *Spiroplectammina spectabilis* in its base, and a more diversified association, comprising *Spiroplectammina* cf. *laevis, Gaudryina healyi, Dorothia elongata, Dorothia paeminosa, Rhizammina algaeformis* and *Marssonella oxycona*, as well as representatives of the genera *Rhabdammina, Cribrostomoides, Bathysiphon* and *Verneuilinoides*. *Spiroplectammina spectabilis* was registered from the Campanian to the Eocene by Charnock and Jones (1990), however, several authors (e.g., Kaminski, 1984; Kaminski et al., 1988; Kaiho, 1992; Bolli et al., 1994; Strong et al., 1995; Koutsoukos, 2000; Alegret et al., 2003; Kaminski and Gradstein, 2005; Alegret and Thomas, 2007; Setoyama et al., 2008; Malumián and Jannou, 2010) have indicated that *S. spectabilis* is a useful Maastrichtian–late Eocene marker. Malumián and Náñez (2012) considered the first appearance of *S. spectabilis* to be a proxy for the base of the Maastrichtian, in assemblages where other age indicators were absent. *Dorothia paeminosa* has been described by Huber (1988) in the Maastrichtian Seymour Island sequence, occurring in low to high abundance. In this study, the species was recorded in the upper part of The Naze, where it occurred in association with *S. spectabilis*, *S.* cf. *laevis*, *G. healyi* and *D. elongata*. The last two species have been used as index fossils for the Haumurian Stage (lower Campanian to upper Maastrichtian) (Webb, 1971, 1973). In the JRI region, their occurrence was restricted to the Campanian sediments, indicating that its distribution was probably environmentally controlled (Huber, 1988). In The Naze, *G. healyi* and *D. elongata* were both recorded in the upper part of the studied section, suggesting that their distribution was facies

Fig. 7. Agglutinated foraminifera from The Naze, section D: A *Rhabdammina* sp.; lateral view, PA29.8; B *Bathysiphon* sp.; lateral view, PA29.7; C *Rhizammina algaeformis*; lateral view, PA29.8; D *Rhizammina* sp.; lateral view, PA29.1; E and I *Saccammina sphaerica* (E lateral view, PA29.7; I lateral view PA29.4); F–G *Thurammina papillata* (F lateral view, PA29.4; G lateral view, PA29.4); H *Rzehakina epigona*; lateral view, PA29.1; J *Reophax texanus*; lateral view, PA29.4; K *Ammodiscus cretaceus*; lateral view, PA29.2; L–M *Haplophragmoides eggeri* (L lateral view, PA29.7; M lateral apertural view, PA29.9); N–P *Haplophragmoides platus* (N dorsal view, PA29.2; O lateral apertural view, PA29.8; P ventral view, PA29.9); Q and U *Labrospira* sp. (Q ventral view, PA29.2; U dorsal view, PA29.2); R and S *Praesphaerammina* sp. (R ventral view, PA29.1; S dorsal view, PA29.1); T *Budashevaella* sp.; ventral view, PA29.7. Scale bar = 100 μm.

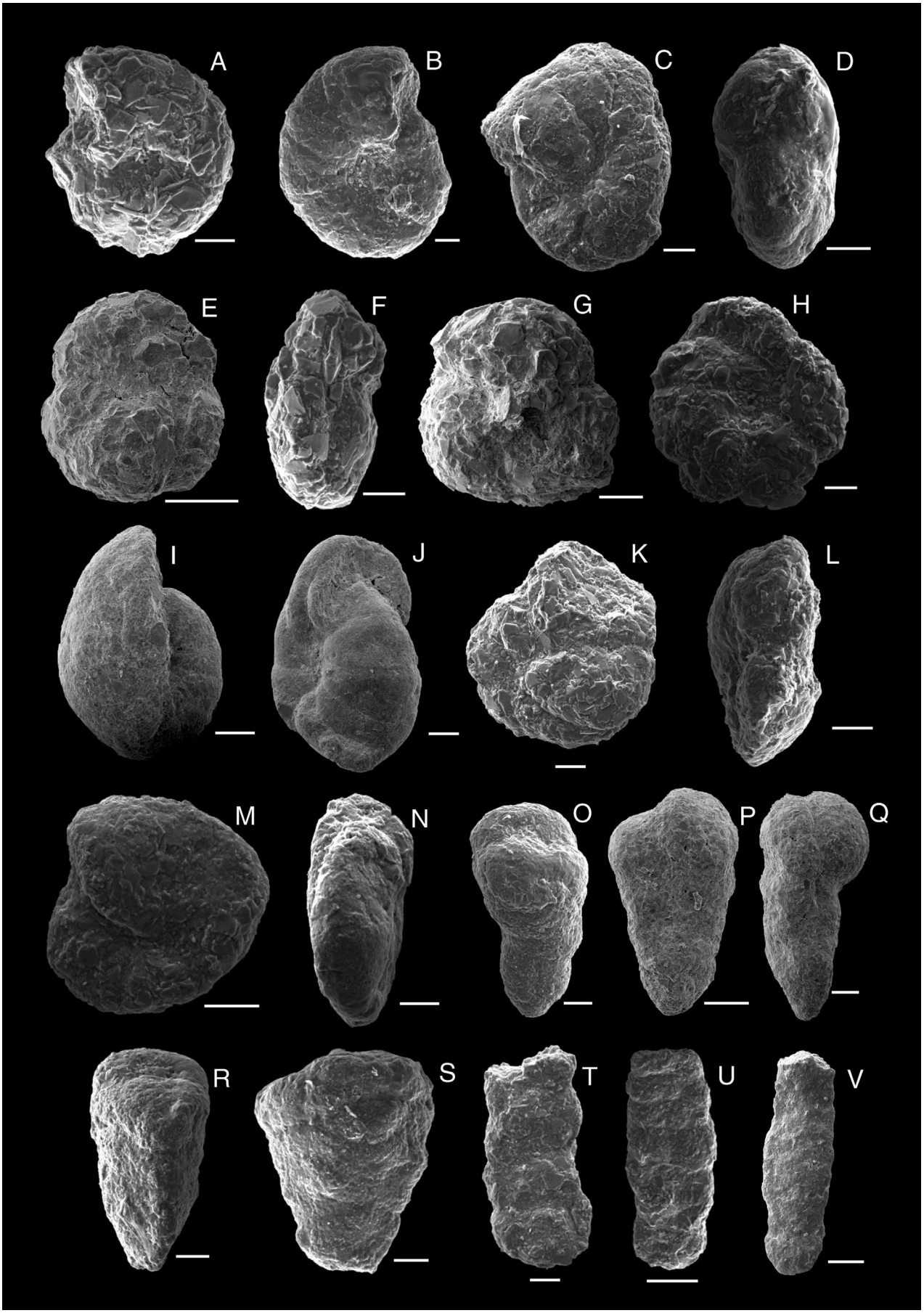
A
B
C
D
E
F
G
H
I
J
K
L
M
N
O
P
Q
R
S
T
U
V

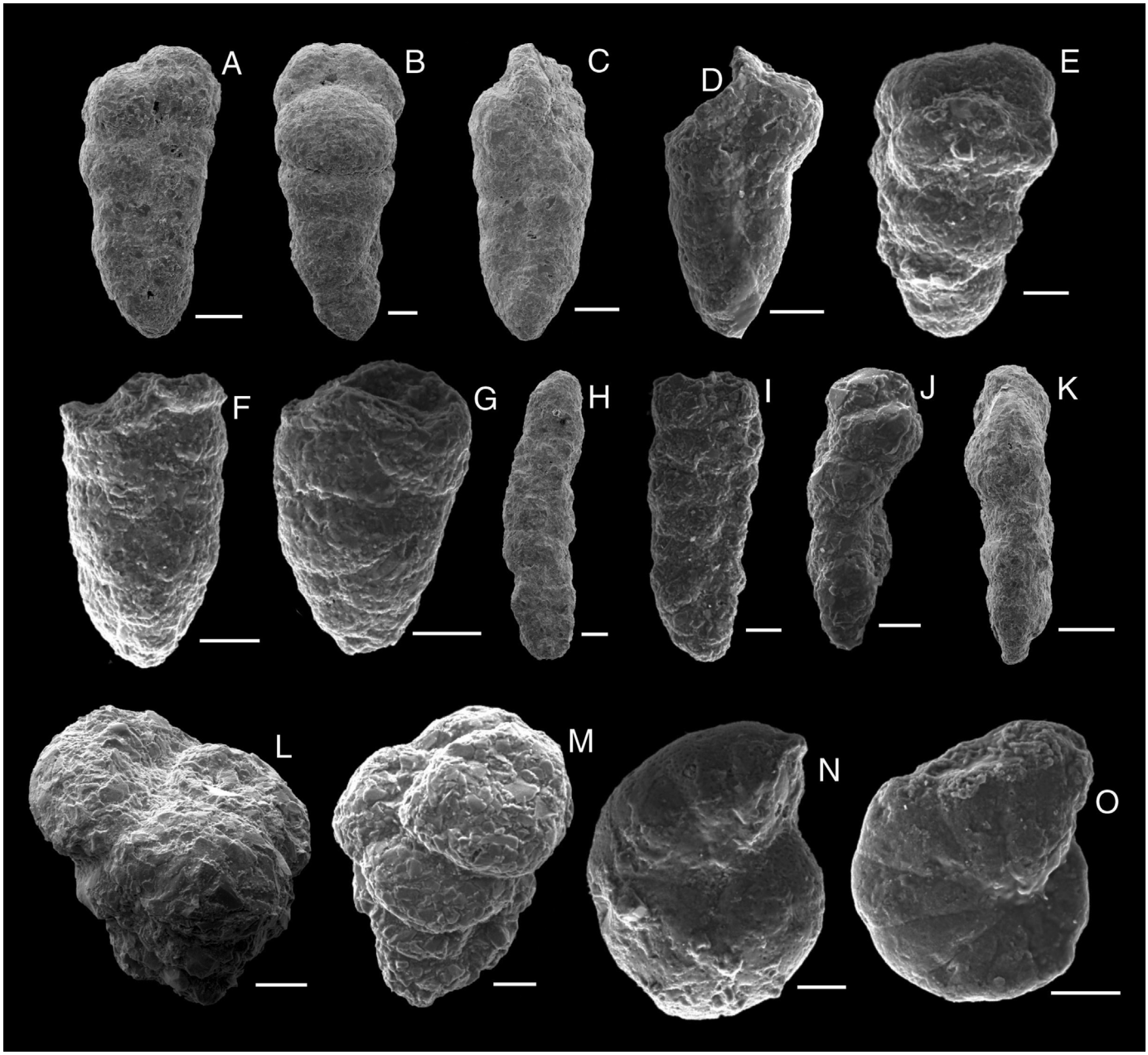

Fig. 9. Agglutinated foraminifera from The Naze, section D: A–C *Dorothia elongata* (A lateral view, PA29.7; B lateral apertural view, PA29.10; C lateral view, PA29.7); D–E *Dorothia paeminosa* (D lateral view, PA29.8; E lateral view, PA29.2); F–G *Marssonella oxycona*; lateral view, PA20.10; H–I *Karreriella aegra* (H lateral view, PA29.7; I lateral view, PA29.4); J–K *Karreriella* sp. (J lateral view, PA29.4; K lateral view, PA29.4); L–M *Verneuilinoides* sp. (L apertural view, PA29.9; M lateral view, PA29.9); N, O *Anomalinoides* sp. (N lateral umbilical view, PA29.2; O lateral umbilical view, PA29.10). Scale bar = 100 μm.

controlled—and that their biostratigraphic value in correlations was limited.

The presence of *R. epigona* at the base of the Naze section, the disappearance of *T. ribstonensis*, and the appearance of *S. spectabilis*, *G. healyi* and *D. paeminosa* in the middle portion of the section (samples PA29.6–8) constituted remarkable bioevents (Fig. 6), which could indicate Campanian–Maastrichtian transition. The appearance of *S. spectabilis* near the Campanian–Maastrichtian boundary was also reported in the Fuegian Andes, Austral Basin (Malumián and Jannou, 2010). In the same way, Lamanna et al. (2019) inferred that the records of the non-avian dinosaurs from the JRB occurred within a relatively condensed temporal interval of

Fig. 8. Agglutinated foraminifera from The Naze, section D: A–B *Cribrostomoides* sp.; lateral view, PA29.10; C–D *Recurvoides* sp. (C lateral view, PA29.2; D lateral apertural view, PA29.2); E–G *Trochammina globigeriniformis* (E ventral view, PA29.7; F lateral view, PA29.4; G dorsal view, PA29.9); H, K, L *Trochammina ribstonensis* (H ventral view, PA29.2; K dorsal view, PA29.10; L lateral view, PA29.2); I, J *Alveolophragmium macellarii* (I lateral view, PA29.7; J lateral view, PA29.10); M–N *Cyclammina complanata* (M ventral view, PA29.2; N lateral view, PA29.2); O–Q *Gaudryina healyi* (O lateral apertural view, PA29.8; P lateral view, PA29.7; Q lateral view, PA29.8); R–S *Spiroplectammina* cf. *laevis* (R lateral apertural view; S lateral view; PA29.4); T–V *Spiroplectammina spectabilis* (T lateral view, PA29.10; U lateral view, PA29.9; V lateral view, PA29.4). Scale bar = 100 μm.

Morphogroup	M1	M2				M3a	M4		
		M2a	M2b		M2c		M4a	M4b	
Morphotype	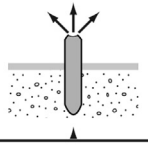	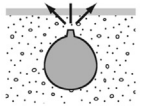	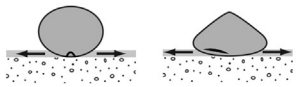		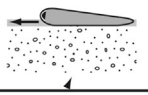		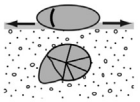	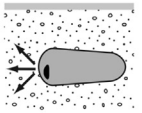	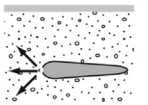
Test Form	Tubular	Globular	Rounded trochospiral and steptospiral	Planoconvex trochospiral	Elongate keeled	Flattened planispiral and steptospiral	Rounded planispiral	Elongate subcylindrical	Elongate tapered
Live position	Erect epifauna	Shallow infauna	Epifauna		Epifauna	Epifauna	Epifauna and/or shallow infauna	Deep infauna	
Feeding habit	Suspension feeding	Suspension feeding and/or passive deposit feeding	Active deposit feeding		Active deposit feeding	Active and passive deposit feeding	Active deposit feeding	Active deposit feeding	
Environment	Tranquil bathyal and abyssal with low organic flux	Common in bathyal and abyssal	Shelf to deep marine		Shelf to marginal marine	Lagoonal to abyssal	Inner shelf to upper bathyal	Inner shelf to upper bathyal with increased organic matter flux	
Genera	*Bathysiphon* *Rhizammina* *Rhabdammina*	*Saccammina* *Praesphraerammina* *Thurammina*	*Cribrostomoides* *Recurvoides*	*Trochammina* *Labrospira* *Budashevaella*	*Spiroplectammina*	*Ammodiscus* *Rzehakina*	*Alveolophragmium* *Haplophragmoides* *Cyclammina*	*Reophax* *Marsonella* *Gaudryina* *Verneulinoides*	*Karreriella* *Dorothia*

Fig. 10. Morphogroups and morphologies of agglutinated foraminifera identified in the studied section (modified from Jones and Charnock, 1985; Nagy et al., 1995, 1997; van den Akker et al., 2000; Kaminski and Gradstein, 2005; Cetean et al., 2010; Murray et al., 2011; Setoyama et al., 2011).

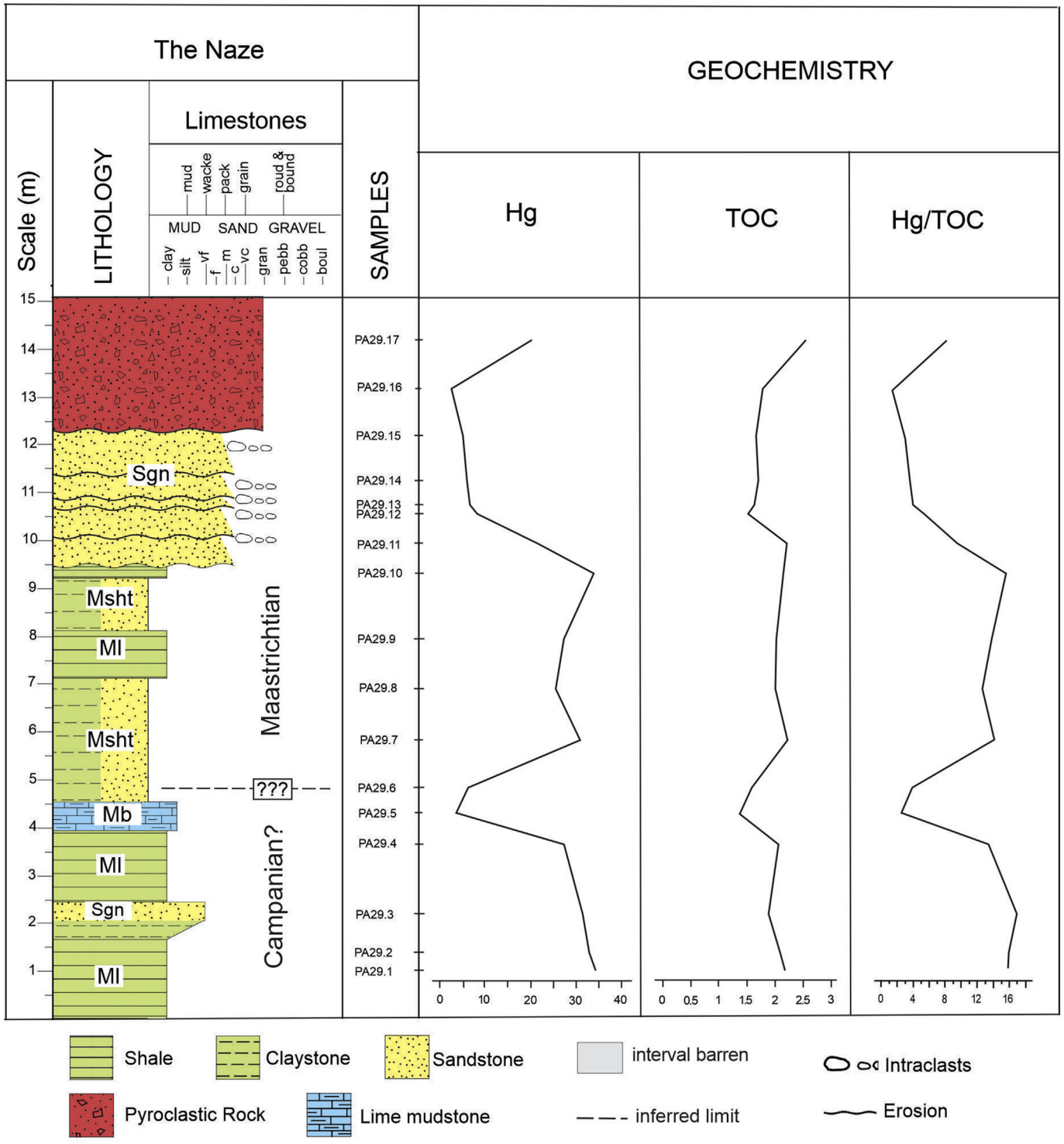

Fig. 11. Total Hg (ng.g^{-1}) and TOC (%) concentrations, and Hg/TOC ratios, along section D of The Naze study area, James Ross Island.

Table 1
Stratigraphic and paleogeographic distribution of the most representative taxa found in this study at The Naze study area, James Ross Island.

Representative taxa	Chronost. horizon	Locality	References
Spiroplectammina spectabilis (Grzybowski, 1898)	Maastrichtian to Paleocene	New Zealand	Strong et al. (1995)
	Maastrichtian to Paleocene	Barents Sea, Arctic Ocean	Setoyama et al. (2008)
	Maastrichtian to Paleocene	Spain	Alegret et al. (2003)
	Maastrichtian to Paleocene	South Atlantic Ocean	Alegret and Thomas (2007)
	Maastrichtian to Eocene	Trinidad	Kaminski et al. (1988)
	Maastrichtian to Eocene	Trinidad	Bolli et al. (1994)
	Maastrichtian to Eocene	Fuegian Andes	Malumián and Jannou (2010)
	Upper Campanian to Maastrichtian	James Ross Island; Vega Island; Seymour Island	Huber (1988)
	Upper Campanian to Paleocene	Italy	Kuhnt and Kaminski (1990)
	Campanian to Eocene	North Sea	Charnock and Jones (1990)
Spiroplectammina cf. *laevis* (Roemer, 1841)	Maastrichtian	Vega Island; Seymour Island	Huber (1988)
Trochammina ribstonensis Wickenden, 1932	Upper Santonian and lower Maastrichtian	Caribbean Sea	Wall (1967)
	Upper Campanian to Maastrichtian	James Ross Island; Seymour Island	Huber (1988)
	Cenomanian to Campanian	Alaska	Tappan (1962)
	Santonian to Campanian	North Atlantic	Cushman (1946); Nauss (1947); Mello (1971); Caldwell and North (1984)
Gaudryina healyi Finlay, 1939	Lower(?) to upper Maastrichtian	Lord Howe Rise	Webb (1973)
	Lower Maastrichtian	Southern Argentina	Malumián and Masiuk (1976)
	Upper Campanian to Maastrichtian	James Ross Island; Vega Island; Seymour Island	Huber (1988)
	Upper Campanian to Maastrichtian	New Zealand	Webb (1971)
Alveolophragmium macellarii Huber, 1988	Upper Campanian to Maastrichtian	James Ross Island; Vega Island; Seymour Island	Huber (1988)
Cyclammina complanata Chapman, 1904	Paleocene to lower(?) Eocene	Southern Australia	Ludbrook (1977)
	Upper Campanian to Maastrichtian	New Zealand	Webb (1971)
	Upper Campanian to Maastrichtian	James Ross Island; Vega Island; Seymour Island	Huber (1988)
Dorothia elongata Finlay, 1940	Lower (?) to upper Maastrichtian	Lord Howe Rise	Webb (1973)
	Upper Campanian to upper Maastrichtian	New Zealand	Webb (1971)
	Upper Campanian to Maastrichtian	The Naze, James Ross Island	Huber (1988)
Dorothia paeminosa Huber, 1988	Maastrichtian	Seymour Island	Huber (1988)
Karreriella aegra (Finlay, 1940)	Upper Campanian to lower Maastrichtian	New Zealand	Webb (1971)
	Upper Campanian to lower Maastrichtian	James Ross Island	Huber (1988)
Rzehakina epigona (Rzehak, 1895)	Maastrichtian to Paleocene	Kamchatka Peninsula, Rússia	Serova (1969)
	Maastrichtian	Sergipe Basin, NE Brazil	Koustoukos (2000)
	Upper Campanian to upper Maastrichtian	James Ross Island	Huber (1988)
	Upper Campanian to upper Maastrichtian	New Zealand	Scott (1961)
	Upper Campanian	Carpathians, Poland	Kostka (1993); Bak (2000))

the late Campanian to early Maastrichtian, including species from The Naze. In our material, however, the absence of planktic foraminifera and specialized benthic forms, which have been useful in dating Upper Cretaceous strata in North America and Europe, prevented more accurate dating. The recovered ammonoids had been reworked, and could not be applied in the biostratigraphic interpretation.

5.2. Paleoenvironmental approach

The paleoenvironmental interpretation based on the distribution of foraminiferal morphogroups and lithofacies indicated a proximal environment. Sgn lithofacies demonstrate high energy, resulting in a drastic reduction in abundance, and Mb lithofacies indicates a lower sea level, associated with infaunal foraminifera. The predominance of morphogroups M4 (*Haplophragmoides, Alveolophragmium, Cyclammina* and *Karreriella*) and M2b (*Trochammina*) (Figs 10 and 12) throughout the section studied indicates a low oxygen environment—and may even tolerate periods of anoxia, adapted to life in eutrophic areas, with higher levels of organic flux (Koutsoukos and Hart, 1990; Nagy et al., 1997; Holbourn et al., 1999; Kaminski and Gradstein, 2005). Both *Trochammina* and *Haplophragmoides* are considered to have been opportunistic taxa, showing tolerance to stressful conditions, such as salinity and oxygen changes. *Haplophragmoides* (epifaunal/infaunal) could move vertically through the sediment, depending on food availability (Jones and Charnock, 1985; Kuhnt and Kaminski, 1990, 1996; Kaminski et al., 1999; Kaminski and Gradstein, 2005; Nagy et al., 2010; Reolid et al., 2014), while *Haplophragmoides* acmes have been related to paleoenvironmental instability events in the Cretaceous–Paleogene transition, in Spain (Alegret et al., 2003).

Above the Mb lithofacies (sample PA29.5), was observed an increase in the M2c morphotypes, represented by specimens of *Spiroplectammina*, which have been considered generally to be shallow water inhabitants, (Nagy et al., 1995, 1997; van den Akker

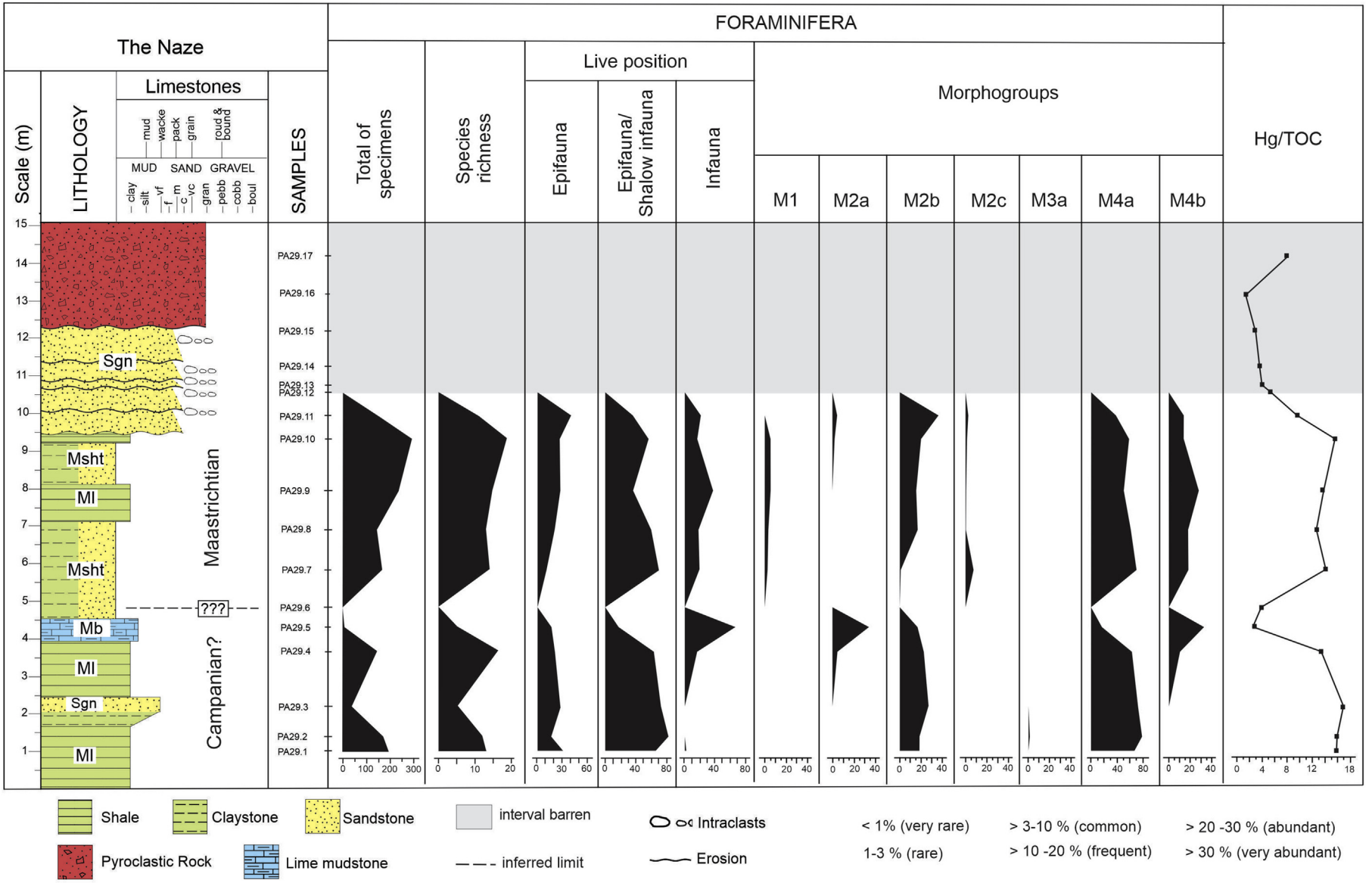

Fig. 12. Integration of lithofacies, micropaleontological and geochemical data from section D of The Naze study area, James Ross Island.

et al., 2000; Kaminski and Gradstein, 2005; Cetean et al., 2010; Setoyama et al., 2011). In addition, *T. ribstonensis* (components of M2 morphogroup) has a small test, which is an adaptation to low oxygen conditions (Reolid et al., 2014), in shallow and somewhat turbid environments (Wall, 1967; Mello, 1971).

In the upper portion of the section (from sample PA29.7), we observed an increase in foraminifera richness, and in the proportion of tubular forms (morphogroup M1) associated with Ml lithofacies, indicating low energy and oxygenation. The recovered association has the characteristic of flysch-type assemblages of the "Type-A" of Gradstein and Berggren (1981), and corresponded to the *Rhabdammina*-fauna of Brouwer (1965), which consisted of large, coarsely agglutinated, simple forms. Tubular forms are rare or absent in a platform environment, since they are adapted to deeper water (Jones and Charnock, 1985; Koutsoukos, 2000; Kaminski and Gradstein, 2005), where they predominate in low organic flux situations (Nagy et al., 1997). On Seymour Island, Huber (1988) identified a similar foraminiferal assemblage in the Maastrichtian, attributed to accumulations from sediment winnowing, or opportunistic blooms occurring during periods of high turbidity and sedimentation.

The Snow Hill Island Formation consists of a gradational coarsening and thickening-upward succession of mudstones and sandstones, represent near-shore facies (e.g., Crame et al., 1991; Pirrie et al., 1991, 1997). Olivero (2012) inferred a low-energy shelf setting for the Campanian–early Maastrichtian to Snow Hill Island Formation deposits, based in sedimentary and ammonite data. In The Naze, foraminiferal distributions indicate an inner neritic environment (Huber, 1988) and the dinoflagellate assemblages supports the general interpretation of a shelf marine deposits (Di Pasquo and Martin, 2013). The data presented here reinforce that the strata of The Naze were deposited in low energy shelf setting, based on the lithological composition and the foraminiferal information.

The observed Hg/TOC negative incursions at the Campanian–Maastrichtian transition were linked to a decrease in organic carbon content and Hg concentrations, which suggested shallower burial or runoff. The CMBE, which occurred from 71.5 Ma to 70 Ma, was caused by a change in intermediate-to deep-water circulation from low-latitude to high-latitude water masses (Koch and Friedrich, 2012). These changes caused cooler temperatures, higher oxygen concentrations, and possibly smaller organic-matter flux to the seafloor—and also induced major changes in the benthic foraminiferal assemblage (Koch and Friedrich, 2012). Notwithstanding these phenomena occurring in deep waters, their resonance on the continental shelf and coastal waters are very likely, as has been demonstrated by oceanographic responses to the present warming of the South Atlantic Ocean over continental shelves (Lacerda et al., 2020; Figueiredo et al., 2020 and references therein).

The Hg/TOC results presented here corroborated events described before and after the CMBE. In the inferred late Campanian, higher Hg and TOC, reflecting increases in both TOC and Hg concentrations, gave rise to lower Hg/TOC ratios at the boundary, confirming global cooling and an oligotrophic ocean with less organic carbon production and deposition. Later, the lower Maastrichtian deposits re-established higher Hg/TOC ratios, which suggested increasing biological production, under the influence of warmer temperatures.

Lithological facies, foraminiferal assemblages, and Hg/TOC values showed clear correlations (Fig. 12). Foraminiferal diversity and abundance peaks were related to positive incursions in Hg/TOC, and to the lithofacies Ml. Although the dominance of opportunistic agglutinated foraminifera clearly demonstrated that the environment in the Late Cretaceous was quite stressful, correlation between the positive Hg/TOC incursions and the greater diversity and abundance of foraminifera were different in recent foraminifera associations, where the main Hg effects consisted of reduced diversity and of morphological abnormalities in their carapaces (Ferraro et al., 2006; Coccioni et al., 2009; Frontalini et al., 2009; Caruso et al., 2011; Frontalini et al., 2018), or the high test fragmentation and dissolution in the fossil planktic foraminifera, as identified in K–Pg transition sections (Font et al., 2016; Punekar et al., 2016). However, studies of recent species have shown that, in some cases, such as the tubular foraminifera *Rhizammina*, organisms can live and even flourish in higher Hg concentrations (Saraswat et al., 2004; Nigam et al., 2009). This occurs possibly due to the notable ecological tolerance of the agglutinated foraminifera to unfavorable conditions—such as low temperatures and oxygen content, variations in salinity, and greater turbidity—in which other organisms cannot survive (Malumián and Náñez, 1990; Koutsoukos and Hart, 1990). The low occurrence of calcareous benthic foraminifera, as well as the absence of planktic forms, can be explained by the influence of diagenetic factors associated with environmental stress (Huber, 1988), which only agglutinated forms could withstand. Therefore, the observed positive association between Hg/TOC and foraminiferal diversity was not causal, but both the increasing Hg concentrations and/or deposition reflected a response to the same environmental drivers, such as changes in salinity and/or turbidity. In addition, the absence of a typical Hg/TOC peak, as observed in other studies, did not support distal drivers, such as volcanism, as being significant causes of environmental change.

6. Conclusions

An association of opportunistic foraminifera taxa, related to a set of four lithofacies, were mapped along The Naze area, JRI, illustrating a predominantly stressful neritic environment. The recorded association of agglutinated foraminifera consist mainly of *R. epigona, T. ribstonensis, G. healyi, K. aegra, D. elongata, A. macellarii, C. complanata* and *S. spectabilis*, that allow to infer a Campanian–early Maastrichtian age to the studied interval. The basal portion of the studied section was marked by the presence of *R. epigona*, *T. ribstonensis*, and low diversity. The upper portion was marked by the first occurrence of *S. spectabilis, G. healyi, D. elongata* and *D. paeminosa*, and was associated with increased diversity and abundance. The strata of The Naze were deposited in low energy shelf setting, based on the lithological composition and the foraminiferal morphogroups.

The Hg, TOC, and Hg/TOC distribution were a response to nutrient input and productivity, suggesting that regional oceanic processes were a major driver of environmental changes, rather than distal sources of environmental stress, such as volcanism.

Acknowledgments

This study was supported by the Programa Antártico Brasileiro - PROANTAR (CNPq #442677/2018-9 to AWAK). The team of the PALEOANTAR Project wants to thank all the NApOc Ary Rongel military group and pilots of the HU-1 helicopter squadron for safely transporting personal and equipment to Antarctica. Alberto Barioni and Nelson Barretta ensured the team's physical integrity during commuting around The Naze on JRI, and also kept the camp running during the expedition at the XXXVI Antarctic Operation. We would like to thank the additional support received from the Conselho Nacional de Desenvolvimento Científico e Tecnológico - CNPq to JMS (#311715/2017-6) and AWAK (#313461/2018-0); Fundação de Desenvolvimento Carlos Chagas Filho de Amparo à Pesquisa do Estado do Rio de Janeiro - FAPERJ to AWAK (#E-26/202.905/2018), Fundação Cearense de Apoio ao Desenvolvimento

Científico e Tecnológico (FUNCAP #BP3-0139-00166.01.00/18 to APP) and Pró-Reitoria de Pesquisa e Pós-Graduação of Universidade Federal de Pernambuco PROPESQ-UFPE for fellowship to JMS and EKP. This study was financed in part by the Coordenação de Aperfeiçoamento de Pessoal de Nível Superior - Brasil (CAPES) - Finance Code 001. The authors thank the anonymous reviewers and the Editor, E.A.M. Koutsoukos, for their suggestions, which allowed us to improve our manuscript significantly.

References

Aguiar, J.E., Marins, R.V., Almeida, M.D., 2007. Comparação de metodologias de digestão de sedimentos marinhos para caracterização da geoquímica de mercúrio. Geochimica Brasiliensis 3 (21), 304–323.

Alegret, L., Molina, E., Thomas, E., 2003. Benthic foraminiferal turnover across the Cretaceous/Paleogene boundary at Agost (southern Spain): paleoenvironmental inferences. Marine Micropaleontology 48 (3–4), 251–279. https://doi.org/10.1016/S0377-8398(03)00022-7.

Alegret, l., Thomas, E., 2007. Deep-Sea environments across the Cretaceous/Paleogene boundary in the eastern South Atlantic Ocean (ODP Leg 208, Walvis Ridge). Marine Micropaleontology 64, 1–17. https://doi.org/10.1016/j.marmicro.2006.12.003.

Amenábar, C.R., Caramés, A., Adamonis, S., Doldan, A., Maceiras, G., Concheyro, A., 2019. Mesozoic and Cenozoic microbiotas from eastern Antarctic Peninsula: adaptation to a changing palaeoenvironment. Advances in Polar Science 30 (3), 165–185. https://doi.org/10.13679/j.advps.2019.0017.

Askin, R.A., 1988. Campanian to Paleocene palynological succession of Seymour and adjacent islands, northeastern Antarctic Peninsula. In: Feldmann, R.M., Woodburne, M.O. (Eds.), Geology and Paleontology of Seymour Island, Antarctic Peninsula, vol. 169. Geol. Soc. Am. Mere., pp. 131–153

Bak, K., 2000. Biostratigraphy of deep-water agglutinated Foraminifera in Scaglia Rossatype deposits of the Pieniny Klippen Belt, Carpathians, Poland. In: Hart, M.B., Kaminski, M.A., Smart, C.W. (Eds.), Proceedings of the Fifth International Workshop on Agglutinated Foraminifera, vol. 7. Grzybowski Foundation Spec. Publ., pp. 15–41

Barrera, E., Savin, S.M., Thomas, E., Jones, C.E., 1997. Evidence for thermohaline-circulation reversals controlled by sea-level change in the latest Cretaceous. Geology 25, 715–718. https://doi.org/10.1130/0091-7613(1997)025<0715:EFTCRC>2.3.CO;2.

Bolli, H.M., Beckmann, J.P., Saunders, J.B., 1994. Benthic foraminiferal biostratigraphy of the south Caribbean region. Cambridge University Press, Cambridge, p. 408. https://doi.org/10.1017/CBO9780511564406.

Bowman, V.C., Francis, J.E., Riding, J.B., Hunter, S.J., Haywood, A.M., 2012. A latest Cretaceous to earliest Paleogene dinoflagellate cyst zonation from Antarctica, and implications for phytoprovincialism in the high southern latitudes. Review of Palaeobotany and Palynology 171, 40–56. https://doi.org/10.1016/j.revpalbo.2011.11.004.

Brouwer, J., 1965. Agglutinated foraminiferal faunas from some turbiditic sequences. I + II. Proceedings koninklijke nederlalldse Akademle vall Wetensclzappen, BB 68, 309–334.

Calabozo, F.M., Strelin, J., Orihashi, Y., Sumino, H., Keller, R.A., 2015. Volcano-ice-sea interaction in the Cerro Santa Marta area, northwest James Ross Island, Antarctic Peninsula. Journal of Volcanology and Geothermal Research 297, 89–108. https://doi.org/10.1016/j.jvolgeores.2015.03.011.

Caldwell, W.G.E., North, B.R., 1984. Cretaceous stage boundaries in the southern Interior Plains of Canada. Bulletin of the Geological Society of Denmark 33, 57–69.

Caramés, A., Amenábar, C.R., Concheyro, A., 2016. Upper Cretaceous foraminifera and palynomorphs from Ekelöf coast section, Ekelöf point, eastern James Ross Island, Antarctic Peninsula. Ameghiniana 53, 333–357. https://doi.org/10.5710/AMGH.27.01.2016.2963.

Caruso, A., Cosentino, C., Tranchina, L., Brai, M., 2011. Response of benthic foraminifera to heavy metal contamination in marine sediments (Sicilian coasts, Mediterranean Sea). Journal of Chemical Ecology 27, 9–30. https://doi.org/10.1080/02757540.2010.529076.

Cetean, C.G., Balc, R., Kaminski, M.A., Filipescu, S., 2010. Integrated biostratigraphy and palaeoenvironments of an upper Santonian–upper Campanian succession from the southern part of the Eastern Carpathians, Romania. Cretaceous Research 32, 575–590. https://doi.org/10.1016/j.cretres.2010.11.00.

Charnock, M., Jones, R.W., 1990. Agglutinated foraminifera from the Palaeogene of the North Sea. In: Hemleben, C., et al. (Eds.), Paleoecology, Biostratigraphy, Paleoceanography and Taxonomy of Agglutinated Foraminifera, pp. 139–244.

Coccioni, R., Frontalini, F., Marsili, A., Mana, D., 2009. Benthic foraminifera and trace element distribution: a case-study from the heavily polluted lagoon of Venice (Italy). Marine Pollution Bulletin 59, 257–267. https://doi.org/10.1016/j.marpolbul.2009.08.009.

Crame, J.A., 1992. Late Cretaceous palaeoenvironments and biotas: an Antarctic perspective. Antarctic Science 4, 371–382. https://doi.org/10.1017/S0954102092000555.

Crame, J.A., Francis, J.E., Cantrill, D.J., Pirrie, D., 2004. Maastrichtian stratigraphy of Antarctica. Cretaceous Research 25, 411–423. https://doi.org/10.1016/j.cretres.2004.02.002.

Crame, J.A., Lomas, S.A., Pirrie, D., Luther, A., 1996. Late Cretaceous extinction patterns in Antarctica. Journal of the Geological Society 153, 503–506. https://doi.org/10.1144/gsjgs.153.4.0503.

Crame, J.A., McArthur, J.M., Pirrie, D., Riding, J.B., 1999. Strontium isotope correlation of the basal Maastrichtian Stage in Antarctica to the European and US biostratigraphic schemes. Journal of the Geological Society. London 156, 957–964. https://doi.org/10.1144/gsjgs.156.5.0957.

Crame, J.A., Pirrie, D., Riding, J.B., Thomson, M.R.A., 1991. Campanian-Maastrichtian (Cretaceous) stratigraphy of the James Ross Island area, Antarctica. Journal of the Geological Society 148, 1125–1140. https://doi.org/10.1144/gsjgs.148.6.1125.

Crampton, J., Mumme, T., Raine, I., Roncaglia, L., Schi⎚ler, P., Strong, P., Turner, G., Wilson, G., 2000. Revision of the Piripauan and Haumurian local stages and correlation of the Santonian-Maastrichtian (Late Cretaceous) in New Zealand. New Zealand Journal of Geology and Geophysics 43 (3), 309–333. https://doi.org/10.1080/00288306.2000.9514890.

Cushman, J.A., 1946. Upper Cretaceous foraminifera of the Gulf Coastal region of the United States and adjacent areas. United States Geological Survey, p. 241p. Professional Paper, 206.

Del Valle, R.A., Fourcade, N.H., Medina, F.A., 1982. The stratigraphy of Cape Lamb and the Naze, Vega and James Ross Islands, Antarctica. In: Craddock, C. (Ed.), Antarctic Geoscience, pp. 275–280. Wisconsin, USA.

Del Valle, R.A., Scasso, R.A., 2004. Límite de la cuenca Larsen en la península Tabarin, Antártida. Revista de la Asociación Geológica Argentina 59 (1), 38–44.

Di Pasquo, M., Martin, J.E., 2013. Palynoassemblages associated with a theropod dinosaur from the Snow Hill Island Formation (lower Maastrichtian) at the Naze, James Ross Island, Antarctica. Cretaceous Research 45, 135–154. https://doi.org/10.1016/j.cretres.2013.07.008.

Ferraro, L., Sprovieri, M., Alberico, I., Lirer, F., Prevedello, L., Marsella, E., 2006. Benthic foraminifera and heavy metals distribution: a case study from the Naples Harbour (Tyrrhenian Sea, Southern Italy). Environmental Pollution 142, 274–287. https://doi.org/10.1016/j.envpol.2005.10.026.

Figueiredo, T.S., Santos, T.P., Costa, K.B., Toledo, F., Albuquerque, A.L.S., Smoak, J.M., Bergquist, B.A., Silva-Filho, Emmanoel V., 2020. Effect of deep Southwestern Subtropical Atlantic Ocean circulation on the biogeochemistry of mercury during the last two glacial/interglacial cycles. Quaternary Science Reviews 239, 106–368. https://doi.org/10.1016/j.quascirev.2020.106368.

Florisbal, L.S., Kochhann, K.G.D., Baecker-Fauth, S., Fauth, G., Viviers, M.C., Carvalho, A.M., Ramos, R.C., 2013. Benthic foraminifera, ostracods and radiolarians from the Lachman Crags Member (Santa Marta Formation), Upper Santonian–Lower Campanian (Upper Cretaceous) of James Ross Island, Antarctica. Revista Brasileira de Paleontologia 16 (2), 181–196. https://doi.org/10.4072/rbp.2013.2.02.

Font, E., Adatte, T., Sial, A.N., Lacerda, L.D., Keller, G., Punekar, J., 2016. Mercury anomaly, Deccan volcanism and the end-Cretaceous mass extinction. Geology 44, 171–174. https://doi.org/10.1130/G37451.1.

Francis, J.E., Crame, J.A., Pirrie, D., 2006. Cretaceous–Tertiary high-latitude palaeoenvironments, James Ross Basin Antarctica. Journal of the Geological Society 258, 1–5. https://doi.org/10.1144/GSL.SP.2006.258.01.01.

Friedrich, O., Herrle, J.O., Wilson, P.A., Cooper, M.J., Erbacher, J., Hemleben, C., 2009. The early Maastrichtian carbon cycle perturbation and cooling event: Implications from the South Atlantic Ocean. Paleoceanography 24 (PA2211), 1–14. https://doi.org/10.1029/2008PA001654.

Friedrich, O., Norris, R.D., Erbacher, J., 2012. Evolution of middle to Late Cretaceous oceans – A 55 m.y. record of Earth's temperature and carbon cycle. Geology 40, 107–110. https://doi.org/10.1130/G32701.1.

Frontalini, F., Buosi, C., Da Pelo, S., Coccioni, R., Cherchi, A., Bucci, C., 2009. Benthic foraminifera as bio-indicators of trace element pollution in the heavily contaminated Santa Gilla lagoon (Cagliari, Italy). Marine Pollution Bulletin 58, 858–877. https://doi.org/10.1016/j.marpolbul.2009.01.015.

Frontalini, F., Greco, M., Di Bella, L., Lejzerowicz, F., Reo, E., Caruso, A., Cosentino, C., Maccotta, M., Scopelliti, G., Nardelli, M.P., Losada, M.T., du Châtelet, E.A., Rodolfo Coccioni, R., Pawlowski, J., 2018. Assessing the effect of mercury pollution on cultured benthic foraminifera community using morphological and eDNA metabarcoding approaches. Marine Pollution Bulletin 129, 512–524. https://doi.org/10.1016/j.marpolbul.2017.10.022.

Ghidella, M.E., Zambrano, O.M., Ferraccioli, F., Lirio, J.M., Zakrajsek, A.F., Ferris, J., Jordan, T.A., 2013. Analysis of James Ross Island volcanic complex and sedimentary basin based on high-resolution aeromagnetic data. Tectonophysics 585, 90–101. https://doi.org/10.1016/j.tecto.2012.06.039.

Gradstein, F.M., Berggren, W.A., 1981. Flysch-type agglutinated foraminiferal assemblages and the Maestrichtian through Paleocene history of the Labrador and North Seas. Marine Micropaleontology 6, 211–268.

Guerra, R.M., Concheyro, A., Lees, J., Fauth, G., Carvalho, M.A., Ramos, R.R.C., 2015. Calcareous nannofossils from the Santa Marta Formation (Upper Cretaceous), northern James Ross Island, Antarctic Peninsula. Cretaceous Research 56, 550–562. https://doi.org/10.1016/j.cretres.2015.06.009.

Haq, B.U., Hardenbol, J., Vail, P.R., 1987. Chronology of fluctuating sea levels since the Triassic. Science 235, 1156–1167.

Hathway, B., 2000. Continental rift to back-arc basin: Jurassic–Cretaceous stratigraphical and structural evolution of the Larsen Basin Antarctic Peninsula.

Journal of the Geological Society London 157, 417–432. https://doi.org/10.1144/jgs.157.2.417.
Holbourn, A., Kuhnt, W., Albani, A.L., Gomez, A.L.R., Herbin, J.P., 1999. Paleoenvironments and paleobiogeography of the Late Cretaceous Casamance transect (Senegal, NW Africa): distribution patterns of benthic foraminifera, organic carbon and terrigenous flux. Neues Jahrbuch für Geologie und Paläontologie - Abhandlungen 212, 335–377. https://doi.org/10.1127/njgpa/212/1999/335.
Hradecká, L., Vodrážka, R., Nývlt, D., 2011. Foraminifera from the Upper Cretaceous of northern James Ross Island (Antarctica): a preliminary report. Czech Polar Reports 1 (2), 88–95. https://doi.org/10.5817/CPR2011-2-8.
Huber, B.T., 1988. Upper Campanian–Paleocene foraminifera from the James Ross Island region, Antarctic Peninsula. Geological Society of America Memoir 169, 163–252. https://doi.org/10.1130/MEM169-p163.
Huber, B.T., Haerwood, D.M., Webb, P.N., 1983. Upper Cretaceous microfossil biostratigraphy of Seymour Island, Antarctic Peninsula. Antarctic Journal of the United States 18, 72–74.
Huber, B.T., Norris, R.D., Macleod, K.G., 2002. Deep-sea paleotemperature record of extreme warmth during the Cretaceous. Geology 30, 23–126. https://doi.org/10.1130/0091-7613(2002)030<0123:DSPROE>2.0.CO;2.
Jenkyns, H.C., Gale, A.S., Corfield, R.M., 1994. Carbon and oxygen-isotope stratigraphy of the English Chalk and Italian Scaglia and its palaeoclimatic significance. Geological Magazine 131, 1–34. https://doi.org/10.1017/S0016756800010451.
Jones, R.W., Charnock, M.A., 1985. "Morphogroups" of agglutinating foraminifera. Their life positions and feeding habits and potential applicability in (paleo) ecological studies. Revue de Paléobiologie 4, 311–320.
Kaiho, K., 1992. A low extinction rate of intermediate-water benthic foraminifera at the Cretaceous/Tertiary boundary. Marine Micropaleontology 18 (1992), 229–259. https://doi.org/10.1016/0377-8398(92)90014-B.
Kaminski, M.A., 1984. Shape variation in *Spiroplectammina spectabilis* (Grzybowski). Acta Palaeontologica Polonica 29 (1–2), 29–49.
Kaminski, M.A., Gradstein, F.M., 2005. Atlas of Paleogene Cosmopolitan Deep-Water Agglutinated Foraminifera, vol. 10. Grzybowski Foundation Spec. Publ.
Kaminski, M.A., Gradstein, P.M., Berggren, W.A., Geroch, S., Beckmann, J.P., 1988. Flysch-type agglutinated foraminiferal assemblages from Trinidad: taxonomy, stratigraphy and paleobathymetry. Abhandlungen der geologischen Bundesanstalt. Wien 41, 155–227.
Kaminski, A.M., Kuhnt, W., Moullade, M., 1999. The evolution and paleobiogeography of abyssal agglutinated foraminifera since the Early Cretaceous. Neues Jahrbuch für Geologie und Paläontologie-Abhandlungen 212 (1–3), 401–439. https://doi.org/10.1127/njgpa/212/1999/401.
Kellner, A.W.A., Costa, F.R., Weinschütz, L.C., Figueiredo, R.G., Souza, G.A., Brum, A.S., Eleutério, L.H.S., Mueller, C.W., Sayão, J.M., 2019. Pterodactyloid pterosaur bones from Cretaceous deposits of the Antarctic Peninsula. Anais da Academia Brasileira de Ciências 91 (2). https://doi.org/10.1590/0001-3765201920191300.
Koch, M.C., Friedrich, O., 2012. Campanian–Maastrichtian intermediate- to deep-water changes in the high latitudes: Benthic foraminiferal evidence. Paleoceanography 27, PA2259. https://doi.org/10.1029/2011PA002259.
Kostka, A., 1993. The age and micro fauna of the Maruszyna Succession (Upper Cretaceous–Palaeogene), Pieniny Klippen Belt, Carpathians, Poland. Studia Geologica Polonica 102, 7–134.
Koutsoukos, E.A.M., 2000. "Flysch-type" foraminiferal assemblages in the Cretaceous of northeastern Brazil. In: Hart, M.B., Kaminski, M.A., Smart, C.W. (Eds.), Proceedings of the Fifth International Workshop on Agglutinated Foraminifera, vol. 7. Grzybowski Foundation Spec. Publ., pp. 243–260
Koutsoukos, E.A.M., Hart, M.B., 1990. Cretaceous foraminiferal morphogroup distribution patterns, palaeocommunities and trophic structures: a case study from the Sergipe Basin, Brazil. Transactions of the Royal Society of Edinburgh Earth Sciences 81, 221–246. https://doi.org/10.1017/S0263593300005253.
Kristjansson, L., Gudmundsson, M.T., Smellie, J.L., McIntosh, W.C., Esser, R., 2005. Palaeomagnetic, 40Ar/39Ar, and stratigraphical correlation of Miocene–Pliocene basalts in the Brandy Bay area, James Ross Island, Antarctica. Antarctic Science 17 (3), 409–417. https://doi.org/10.1017/s0954102005002853.
Kuhnt, W., Kaminski, M.A., 1990. Paleoecology of Late Cretaceous to Paleocene deep-water agglutinated foraminifera from the North Atlantic and Western Tethys. In: Hemleben, C., Kaminski, M.A., Kuhnt, W., Scott, D.B. (Eds.), Paleoecology, Biostratigraphy, Paleoceanography and Taxonomy of agglutinated foraminifera, vol. 327. Kluwer Academic Press, pp. 433–506.
Kuhnt, W., Kaminski, M.A., 1996. The response of benthic foraminifera to the K/T boundary event - a review. Bulletin des Centres de Recherches Exploration - Production Elf-Aquitaine. 16, 433–442.
Lacerda, L.D., Marins, R.V., Dias, F.J.S., 2020. An Arctic Paradox: Response of fluvial Hg inputs and its bioavailability to global climate change in an extreme coastal environment. Frontiers of Earth Science 8, 1–12. https://doi.org/10.3389/feart.2020.00093.
Lamanna, C.M., Case, J.A., Roberts, E.M., Arbour, V.M., Ely, R.C., Salisbury, S.W., Clarke, A., Malinzak, E., West, A.R., Connor, P.M., 2019. Late Cretaceous non-avian dinosaurs from the James Ross Basin, Antarctica: description of new material, updated synthesis, biostratigraphy, and paleobiogeography. Advances in Polar Science 30, 228–250. https://doi.org/10.13679/j.advps.2019.0007.
Li, L., Keller, G., 1999. Variability in Late Cretaceous climate and deep water: Evidence from stable isotopes. Marine Micropaleontology 161, 171–190. https://doi.org/10.1016/S0025-3227(99)00078-X.
Linnert, C., Robinson, S.A., Lees, J.A., Pérez-Rodríguez, I., Hugh, C., Jenkyns, H.C., Petrizzo, M.R., Arz, J.A., Bown, P.R., Falzoni, F., 2018. Did Late Cretaceous cooling trigger the Campanian–Maastrichtian Boundary Event? Newsletters on Stratigraphy 51 (2), 145–166. https://doi.org/10.1127/nos/2017/0310.
Ludbrook, N.H., 1977. Early Tertiary *Cyclammina* and *Haplophragmoides* (Foraminiferida: Lituolidae) in southern Australia. Transactions of the Royal Society of South Australia 101 (7), 165–198.
Macfadyen, W.A., 1966. Foraminifera from the Upper Cretaceous of James Ross Island. British Antarctic Survey Bulletin 8, 75–87.
Malumián, N., Jannou, G., 2010. Los Andes Fueguinos: el registro micropaleontológico de los mayores acontecimientos paleooceanográficos australes del Campaniano al Mioceno. Andean Geology 1–26. https://doi: 10.5027/andgeoV37n2-a05.
Malumián, N., Masiuk, V., 1976. Foraminíferos de la Formacion Cabeza de León (Cretacico Superior), Tierra del Fuego, Rep. Argentina. Revista de la Asociación Geológica Argentina 31 (3), 180–221.
Malumián, N., Náñez, C., 1990. Foraminíferos Aglutinados Cretácico Superior de Cuenca Austral (Provincia de Santa Cruz) Argentina. In: Volkheimer, W. (Ed.), Bioestratigrafía de los sistemas Regionales del Jurásico y Cretácico de América del Sur, pp. 497–551.
Malumián, N., Náñez, C., 2012. Cretaceous–Paleogene agglutinated foraminifera from the Magallanes or Austral Basin, southernmost South America. In: Alegret, Ortiz, Kaminski (Eds.), 2012. Ninth International Workshop on Agglutinated Foraminifera, pp. 51–53. Abstract Volume.
Mello, J., 1971. Foraminifera from the Pierre Shale (Upper Cretaceous) at Red Bird, Wyoming. Geological Survey Professional Paper 3937C, 73. https://doi.org/10.3133/pp393C.
Mendonça, E.S., Matos, E.S., 2005. Matéria orgânica do solo; métodos de análises. UFV, Viçosa, p. 107.
Milanese, F.N., Olivero, E.B., Raffi, M.E., Franceschinis, P.R., Gallo, L.C., Skinner, S.M., Mitchell, R.N., Kirschvink, J., Rapalini, A., 2019. Mid Campanian–Lower Maastrichtian magnetostratigraphy of the James Ross Basin, Antarctica: Chronostratigraphical implications. Basin Research 31, 562–583. https://doi.org/10.1111/bre.12334.
Morlotti, E., Concheyro, A., 1999. Paleoecological observations on the Upper Cretaceous benthic foraminifera assemblages of Punta Ekelöf, James Ross Island, Antarctica. In: Boletim do 5° Simpósio sobre o Cretáceo de Brasil. UNESP, Campus de Rio Claro/SP, pp. 375–381.
Murray, J.W., Alve, E., Jones, B.W., 2011. A new look at modern agglutinated benthic foraminiferal morphogroups: their value in palaeoecological interpretation. Palaeogeography, Palaeoclimatology, Palaeoecology 309, 229–241. https://doi.org/10.1016/j.palaeo.2011.06.006.
Nagy, J., Gradstein, F.M., Kaminski, M.A., Holbourn, A.E., 1995. Foraminiferal morphogroups, paleoenvironments and new taxa from Jurassic to Cretaceous strata of Thakkhola, Nepal. In: Kaminski, M.A., Geroch, S., Gasinski, M.A. (Eds.), Proceedings of the Fourth International Workshop on Agglutinated Foraminifera, vol. 3. Grzyb. Found. Spec. Pub., pp. 181–209
Nagy, J., Hess, S., Alve, E., 2010. Environmental significance of foraminiferal assemblages dominated by small-sized *Ammodiscus* and *Trochammina* in Triassic and Jurassic delta-influenced deposits. Earth-Science Reviews 99, 31–49. https://doi.org/10.1016/j.earscirev.2010.02.002.
Nagy, J., Kaminski, M.A., Johnsen, K., Mitlehner, A.G., 1997. Foraminiferal, palynomorph, and diatom biostratigraphy and paleoenvironments of the Tork Formation: a reference section for the Paleocene–Eocene transition in the western Barents Sea. In: Hass, H.C., Kaminski, M.A. (Eds.), Contributions to the Micropaleontology and Paleoceanography of the Northern North Atlantic, vol. 5. Grzybowski Foundation Spec. Publ, pp. 15–38.
Nauss, A., 1947. Cretaceous microfossils of the Vermilion area, Alberta. Journal of Paleontology 21 (4), 329–343.
Nigam, V.N., Linshy, S.R., Kurtarkar, R., Saraswat, S.R., 2009. Effects of sudden stress due to heavy metal mercury on benthic foraminifer *Rosalina leei*: laboratory culture experiment. Marine Pollution Bulletin 59, 362–368. https://doi.org/10.1016/j.marpolbul.2009.08.014.
ÓGorman, J.P., 2012. The oldest elasmosaurs (Sauropterygia, Plesiosauria) from Antarctica, Santa Marta Formation (upper Coniacian? Santonian–upper Campanian) and Snow Hill Island Formation (upper Campanian–lower Maastrichtian), James Ross Island. Polar Research 31, 1–10. https://doi.org/10.3402/polar.v31i0.11090.
Odin, G.S., Hancock, J.M., Antonescu, E., Bonnemaison, M., Caron, M., Cobban, W.A., Dhondt, A., Gaspard, D., Ion, J., Jagt, J.W.M., Kennedy, W.J., Melinte, M., Néraudeau, D., von Salis, K., Ward, P.D., 1996. Definition of a Global Boundary Stratotype Section and Point for the Campanian/Maastrichtian boundary. Bulletin de l'Institut Royal des Sciences Naturelles de Belgique, Sciences de la Terre 66 (Suppl. l), 111–117.
Ogg, J.G., Ogg, G.M., Gradstein, F.M., 2016. A Concise Geologic Time Scale. Elsevier B.V, p. 229. https://doi.org/10.1016/B978-0-444-59467-9.00001-7.
Olivero, E.B., 2012. Sedimentary cycles, ammonite diversity and palaeoenvironmental changes in the upper Cretaceous Marambio Group, Antarctica. Cretaceous Research 34, 348–366. https://doi.org/10.1016/j.cretres.2011.11.015.
Olivero, E.B., Medina, F.A., 2000. Patterns of Late Cretaceous ammonite biogeography in southern high latitudes: The Family Kossmaticeratidae in Antarctica. Cretaceous Research 21, 269–279. https://doi.org/10.1006/cres.1999.0192.
Percival, L.M.E., Witt, M.L.I., Mather, T.A., Hermoso, M., Jenkyns, C., Hesselbo, S.P., Alsuwaidi, A.H., Storma, M.S., Xu, W., Ruhla, M., 2015. Globally enhanced Mercury deposition during the end-Pliensbachian extinction and Toarcian OAE: a link to the Karoo-Ferrar Large Igneous Province. Earth and Planetary Science Letters 428, 267–280. https://doi.org/10.1016/j.epsl.2015.06.064.

Pirrie, D., Crame, J.A., Lomas, S.A., Riding, J.B., 1997. Late Cretaceous stratigraphy of the Admiralty Sound region, James Ross Basin, Antarctica. Cretaceous Research 17, 109–137. https://doi.org/10.1006/cres.1996.0052.

Pirrie, D., Crame, J.A., Riding, J.B., 1991. Late Cretaceous stratigraphy and sedimentology of Cape Lamb, Vega Island, Antarctica. Cretaceous Research 12, 227–258. https://doi.org/10.1016/0195-6671(91)90036-C.

Punekar, J., Keller, G., Khozyem, H., Adatte, T., Font, E., Spangenberg, J., 2016. A multiproxy approach to decode the end-Cretaceous mass extinction. Palaeogeography, Palaeoclimatology, Palaeoecology 441, 116–136. https://doi.org/10.1016/j.palaeo.2015.08.025.

Reolid, M., Nikitenko, B.L., Glinskikh, L., 2014. *Trochammina* as opportunist foraminifera in the Lower Jurassic from north Siberia. Polar Research 33, 21653. https://doi.org/10.3402/polar.v33.21653.

Riding, J.B., 1996. A palynological investigation of eight samples from outcrops at Sobral Peninsula, Crabeater Point and Mount Charity, Antarctic Peninsula (Unpublished). British Geological Survey, p. 7. Technical Report WH/96/232R.

Rinaldi, C.A., Massabie, A., Morelli, J., Rosenman, H.L., Del Valle, R.A., 1978. Geologia de la isla Vicecomodoro Marambio. Contribución del Instituto Antártico Argentino 217, 1–44.

Sanei, H., Grasby, S.E., Beauchamp, B., 2012. Latest Permian mercury anomalies. Geology 40 (1), 63–66. https://doi.org/10.1130/G32596.1.

Saraswat, R., Kurtarkar, S.R., Mazumder, A., Nigam, R., 2004. Foraminifers as indicators of marine pollution: a culture experiment with *Rosalina leei*. Marine Pollution Bulletin 48, 91–96. https://doi.org/10.1016/S0025-326X(03)00330-8.

Scott, G.H., 1961. Contribution to the knowledge of *Rzehakina* Cushman (Foraminifera) in New Zealand. New Zealand Journal of Geology and Geophysics 4, 3–43.

Serova, M.Y., 1969. Comparison of characteristics of Rzehakinidae in the Carpathian region and Pacific Province. Rocznik Polskiego Towarzystwa Geologicznego 39, 225–240.

Setoyama, E., Kaminski, M.A., Tyszka, J., 2011. The Late Cretaceous–Early Paleocene palaeobathymetric trends in the southwestern Barents Sea - Palaeoenvironmental implications of benthic foraminiferal assemblage analysis. Palaeogeography, Palaeoclimatology, Palaeoecology 30, 44–58. https://doi.org/10.1016/j.palaeo.2011.04.021.

Setoyama, E., Kaminski, M.A., Tyszka, J., 2008. Late Cretaceous Agglutinated Foraminifera and Implications for the Biostratigraphy and Palaeobiogeography of the southwestern Barents Sea. In: Kaminski, M.A., Filipescu, S. (Eds.), 2011. Proceedings of the Eighth International Workshop on Agglutinated Foraminifera, vol. 16. Grzybowski Foundation Spec. Publ., pp. 251–309

Sial, A.N., Chen, J., Lacerda, L.D., Frei, R., Tewari, V.C., Pandit, M.K., Gaucher, C., Ferreira, V.P., Cirilli, S., Peralta, S., Korte, C., Barbosa, J.A., Pereira, N.S., 2016. Mercury enrichments and Hg isotopes in Cretaceous–Paleogene boundary successions: links to volcanism and palaeoenvironmental impacts. Cretaceous Research 66, 60–81. https://doi.org/10.1016/j.cretres.2016.05.006.

Sial, A.N., Lacerda, L.D., Ferreira, V.P., Frei, R., Marquillas, R.A., Barbosa, J.A., Gaucher, C., Windmöller, C.C., Pereira, N.S., 2013. Mercury as a proxy for volcanic activity during extreme environmental turnover: The Cretaceous–Paleogene transition. Palaeogeography, Palaeoclimatology, Palaeoecology 387, 153–164. https://doi.org/10.1016/j.palaeo.2013.07.019.

Strong, C.P., Hollis, C.J., Wilson, G.J., 1995. Foraminiferal, radiolarian and dinoflagellate biostratigraphy of Late Cretaceous to Middle Eocene pelagic sediments (Muzzle Group), Mead Stream, Marlborough, New Zealand. New Zealand Journal of Geology and Geophysics 38, 171–212. https://doi.org/10.1080/00288306.1995.9514649.

Tappan, H., 1962. Foraminifera from the Arctic Slope of Alaska. Geological Survey Professional Paper 236–C, 189.

van den Akker, T.J.H.A., Kaminski, M.A., Gradstein, F.M., Wood, J., 2000. Campanian to Palaeocene biostratigraphy and palaeoenvironments in the Foula Sub-basin, west of the Shetland Islands, UK. Micropalaeontology 19 (1), 23–43. https://doi.org/10.1144/jm.19.1.23.

Wall, D., 1967. Fossil microplankton in deep-sea cores from the Caribbean Sea. Palaeontology 10, 95–123.

Webb, P.N., 1971. New Zealand Late Cretaceous (Haumurian) foraminifera and stratigraphy: a summary. New Zealand Journal of Geology and Geophysics 14 (4), 795–828.

Webb, P.N., 1972. Comments on the reported occurrence of *Globotruncana contusa* (Cushman) from the Upper Cretaceous of James Ross Island, Grahamland, Antarctica. New Zealand Journal of Geology and Geophysics 15 (1), 183–183.

Webb, P.N., 1973. Upper Cretaceous–Paleocene foraminifera from Site 208 (Lord Howe Rise, Tasman Sea), DSDP, Leg 21, p. In: Burns, R.E., Andrews, J., et al. (Eds.), Initial Reports of the Deep-Sea Drilling Project, vol. 21. U.S. Government Printing Office, Washington, D.C, pp. 541–573.

Yeomans, J.C., Bremner, J.M., 1988. A rapid and precise method for routine determination of organic carbon in soil. Communications in Soil Science and Plant Analysis 19 (1), 1467–1476. https://doi.org/10.1080/00103628809368027.

Appendix A. Supplementary data

Supplementary data to this article can be found online at https://doi.org/10.1016/j.cretres.2020.104725.